Am J Cancer Res 2020;10(10):3138-3156
www.ajcr.us /ISSN:2156-6976/ajcr0116573

Original Article

SHCBP1 regulates STAT3/c-Myc signaling activation to promote tumor progression in penile cancer

Miao Mo[1], Shiyu Tong[1], Hongling Yin[2], Zhongyuan Jin[2], Xiongbing Zu[1], Xiheng Hu[1]

Departments of [1]Urology, [2]Pathology, Xiangya Hospital, Central South University, Changsha 410008, China

Received June 18, 2020; Accepted September 19, 2020; Epub October 1, 2020; Published October 15, 2020

Abstract: A challenge in developing novel strategies for penile cancer (PC) is the limited understanding of the regulatory mechanisms involved in PC development. This study aims to examine the expression of SHC SH2 Domain-Binding Protein 1 (SHCBP1) in PC and to explore its oncogenic function. Aberrant SHCBP1 expression was observed in PC tissues compared with normal penile tissues. SHCBP1 expression was significantly associated with the pathological grade, T stage, nodal status, and pelvic lymph node metastasis, and could serve as an independent factor for unfavorable overall survival in PC. Manipulation of SHCBP1 expression affected cell proliferation, soft agar clonogenesis, and cell migration and invasion in PC cell lines. Moreover, we identified STAT3/c-Myc signaling as a potential downstream target of SHCBP1. SHCBP1 interacted with JAK2 and STAT3 upon EGF stimulation, which might regulate STAT3/c-Myc signaling activation in PC cells. Disruption of STAT3/c-Myc signaling attenuated cell proliferation and cell migration/invasion in PC cell lines. Nevertheless, overexpression of constitutively activated STAT3 or c-Myc rescued cell proliferation and cell migration/invasion caused by SHCBP1 depletion in PC cell lines. Consistently, SHCBP1 depletion attenuated STAT3/c-Myc signaling and suppressed tumor growth in a murine xenograft model. Importantly, correlated expression of SHCBP1, p-STAT3, and c-Myc was observed in PC tissues, confirming the clinical relevance of SHCBP1/STAT3/c-Myc signaling in PC. In conclusion, aberrant SHCBP1 expression could serve as a potential prognostic biomarker for PC. SHCBP1 might activate the STAT3/c-Myc signaling pathway to promote tumor progression in PC, which may serve as a potential target for PC treatment.

Keywords: Penile cancer, SHCBP1, STAT3, c-Myc, prognosis, tumor progression

Introduction

Penile cancer (PC) is a rare malignancy in the United States (0.5-1.6 per 100,000 men), with a significantly higher incidence-up to 20-30 times greater- in some regions of Africa, Asia, and South America [1]. Currently, a surgical operation is recommended as the major treatment for PC. Besides the surgical approach, brachytherapy, chemotherapy, and targeted therapy have also been applied in the clinical management of PC [2, 3]. Although patients with early-stage disease have an estimated 10-year survival of 89%, patients with advanced disease have only an estimated survival of 21% at two years [4]. The clinical outcomes of PC are associated with tumor grade, pathological subtype, human papillomavirus (HPV) status, and clinical stage, with the presence of inguinal nodal metastases being the most important prognostic factor for patient survival [5]. Despite considerable progress in clinical treatment, the survival of patients with PC has not improved in the past 20 years [6].

A challenge in developing novel strategies for PC is the limited understanding of the heterogeneity of the oncogenic drivers of disease. Although HPV infection is a significant contributing factor for PC [7], an extended list of mechanisms responsible for PC has also been documented. Genomic profiling identified clinically relevant genomic alterations of oncogenes and tumor suppressors, with TP53, CDKN2A, PIK3CA, and HRAS among the most frequently altered genes [8]. Nevertheless, hyperactivation of oncogenic pathways such as *EGFR*/RAS, Wnt/β-Catenin, and PI3K/AKT/mTOR, dysregulated DNA methylation, and overexpression of miRNAs were also shown to be involved in PC development [9-12]. Recently, we showed that ID1 and CEACAM19 are closely connected to tumor progression in patients with PC [13, 14]. Despite this aforementioned progress in the PC

study, there is still a limited understanding of the biological regulators of prognostic and therapeutic importance in penile cancer. Further knowledge on the molecular mechanisms underlying PC progression may help in the development of therapeutic strategies.

SHC SH2 Domain-Binding Protein 1 (*SHCBP1*) was initially identified as a potential gene associated with cell proliferation in fibroblasts [15, 16]. *SHCBP1* exerts a crucial physiological function in normal tissue development. Chen et al. showed that *SHCBP1* is an essential component of FGF signaling in neural progenitor cells [17]. *SHCBP1* is also upregulated during T cell proliferation and regulates $CD4^+$ T cell effector function *in vivo* [18]. Recently, *SHCBP1* was shown to be closely associated with cancer development. Aberrant *SHCBP1* expression is associated with poor prognosis and aggressive phenotype in gastric, prostate, and breast cancer [19-24]. However, the expression and oncogenic role of *SHCBP1* in PC remain mostly unknown. Here, we sought to determine the association between *SHCBP1* expression and clinicopathological characteristics of PC and to explore its oncogenic function in PC tumorigenesis.

Materials and methods

Patient and tumor characteristics

Archival paraffin-embedded PC tissues (n = 105) were collected for immunohistochemistry. The PC patients included in this study had complete patient and tumor characteristics, and underwent surgery for PC between 2012 and 2014 at Xiangya Hospital, Central South University. Patients with known chemotherapy or brachytherapy before the surgery were excluded from the study. TNM staging was assigned based on the American Join Committee on Cancer, 8th edition [25]. The study protocols were approved by the research ethics committee in Xiangya hospital (Rev No. 201805847) with informed consent obtained from all patients. Cancer and vital status were determined by clinical follow-up at our institution.

Reagents and cell lines

Primary antibody against *SHCBP1* was kindly provided by Proteintech (Rosemont, IL, USA). Primary antibodies against p-*STAT3* (Tyr705), *STAT3*, *c-Myc*, *JAK2*, cleaved caspase-3 and β-actin were obtained from Cell Signaling Technology (Beverly, MA USA); Human penile cancer cell lines PenI1, PenI2, 149RCa and LM156 were kindly provided by Prof. Hui Han (Department of Urology, Cancer hospital, Sun Yat-sen University) [26]. These cell lines was cultured in Dulbecco's modified Eagle's medium supplemented with 10% fetal bovine serum (Hyclone, Logan, UT, USA), 4 mM glutamine, 100 U/mL penicillin, and 100 μg/mL streptomycin. Lentiviral plasmids expressing shRNAs targeting *SHCBP1*, *STAT3*, or *c-Myc* were purchased from Genecopoeia Inc. (Rockville, MD, USA). Lentiviral LV105 plasmids expressing empty vector (EV), *c-Myc* or *SHCBP1* were purchased from Genecopoeia Inc. (Rockville, MD, USA). Lentiviral plasmids Flag-tagged *STAT3*DN (dominant negative, #24984) and *STAT3*CA (constitutively active, #24983) were provided by Addgene (Watertown, MA, USA). The packaging procedure for lentiviral particles was conducted as we described previously [13, 14].

Cell growth analysis

Cell growth was measured by CCK-8 assay as we described previously [13]. The CCK-8 absorbance (OD_{450}) was measured with a MK3 microplate reader (Thermo Scientific, USA).

Soft agar assay

Soft agar assay was used to examine the *in vitro* clonogenesis of PC cells as described previously [27]. Briefly, the 2 mL culture medium with 0.5% agar was first plated into each well of a 6 cm culture dish. After the agar solidified, each well received another 2 mL of 0.35% agar in culture medium containing 2×10^4 cells. After 2 weeks, colonies were counted. The number of colonies was determined microscopically by manually counting from triplicate wells for each cell line.

Wound healing assay

Cell migration ability was measured by wound healing assay as we described previously [14]. Briefly, after PC cells were grown fully confluent, a uniform scratch was made for each experiment group. The distance between the wound sides was measured immediately after the scratch or after indicated time interval.

Transwell invasion assay

Cell invasion assay were performed based on transwell chamber with 8 μm pores as described previously [28]. Briefly, PC cells were suspended in DMEM medium at 5 × 10^5 cells/ml. Each transwell of 24-well plate was precoated with 50 μl Matrigel. RPMI 1640 medium (600 μl) containing 10% FBS was added to each well (lower compartment), and 0.1 ml (0.5 × 10^5 cells) of cell suspension was added onto each transwell insert (upper compartment). The plates were incubated for 24 h at 37°C. The invaded cells on the bottom surface of the membrane were fixed by 4% paraformaldehyde, and stained by 0.2% crystal violet solution (Sigma-Aldrich, USA). After the wash, cells were photographed with Olympus BX43 microscope. Then the stained cells were eluted by 20% glacial acetic acid and measured with MK3 microplate reader (Thermo Scientific, USA) at 570 nm.

Western blotting

Cell lysates were prepared with RIPA cell lysis buffer. The experimental procedure of Western blotting was conducted as we described previously [13]. Protein blots were visualized using the ECL system (Abcam, Cambridge, MA, USA).

Luciferase reporter assay

Luciferase reporter assay was conducted to examine cancer-related pathway activity as described previously [27]. Briefly, PC cells were grown in 96-well plate and transfected with plasmid construct of transcription factor-responsive reporter of each pathway. After 48 hours, the changes in expression of each pathway in cells with or without *SHCBP1* knockdown were determined by measuring the generated firefly and Renilla luminescent signals using the Dual-Glo Luciferase Assay system (Promega, Madison, WI, USA). The luciferase activity of scramble shRNA control was regarded as 100%.

Co-immunoprecipitation

Co-immunoprecipitation of *SHCBP1* or *JAK2* from PC cell lysates was carried out as described previously [27]. *SHCBP1* and *JAK2* were immunoprecipitated using a rabbit anti-*SHCBP1* or anti-*JAK2* antibody. Rabbit IgG were used as negative controls. Immune complexes were captured using the Protein G Dynabeads (Beyotime Biotechnology), and immunoprecipitates were analyzed by SDS-PAGE followed by immunoblotting with mouse monoclonal anti-*SHCBP1* antibody (Abnova) and mouse monoclonal anti-*STAT3* or anti-*JAK2* antibody (Cell Signaling). Immunoreactive bands were visualized using enhanced chemiluminescence.

Immunohistochemistry (IHC)

Immunohistochemistry on PC tissue sections (n = 105) were performed as we described previously [13, 14]. Briefly, the sections were dewaxed in xylene, rehydrated with graded alcohols and subjected to heat induced epitope retrieval. The sections were then incubated overnight at 4°C with primary antibodies (dilution: *SHCBP1*: 1:200; p-*STAT3*: 1:100; *c-Myc*: 1:200; Ki-67: 1:500), followed by incubation with a horseradish peroxidase conjugated goat anti rabbit secondary antibody (DAKO, Denmark) for 30 min at room temperature. Antigen-antibody reactions were visualized by exposure to 3,3-diaminobenzidine and hydrogen peroxide chromogen substrate (DAKO, Denmark). The staining positivity ≥ 30% was regarded as high expression [13, 14]. IHC results were examined and scored by two pathologists (H.Y and Z.J).

RNA sequencing

RNA sequencing was conducted to identify gene mRNA expression in Penl2 cells transfected with shRNAs targeting *SHCBP1* or *STAT3*. The mRNA libraries were constructed using NEB Next Ultra II Directional RNA Library Prep Kit (Ipswich, MA, USA). High-throughput sequencing was performed on an Illumina HiSeq 4000 platform. Expression levels of each protein-coding gene were expressed as Fragments per kilobase of transcript per million fragments mapped (FPKM). The analysis of differentially expressed genes (DEGs) is performed with the Limma package [29]. Genes meeting the cutoff criteria (adjusted $P < 0.05$ and $|\log_2 FC| \geq 1$) are reported as DEGs.

Pathway and process enrichment analysis

Pathway and process enrichment analysis was conducted in *Metascape* (http://metascape.org/gp/index.html) with ontology sources for GO Biological Processes and KEGG Pathway [30].

GEO dataset

GEO dataset GSE57955 could be downloaded from NCBI GEO website (https://www.ncbi.nlm.nih.gov/geo/query/acc.cgi?acc=GSE57955). Gene expression data were analyzed as described previously [31]. Genes with a mean $\log_2$ signal ratio (penile cancer/normal penile tissue pool) of ≥ 2.0 and ≤ -2.0 were considered differentially expressed.

Gene set enrichment analysis (GSEA)

GSE57955 dataset was used for GSEA analysis. Gene expression profiles were compared between *SHCBP1*-high (n = 20) and *SHCBP1*-low PC (n = 19) based on enrichment of KEGG pathway signatures [32]. The nominal *p* value (NOM *p*-val) and false discovery rate (FDR)-corrected q value (FDR q-val) are indicated. A nominal *P* value of < 0.05 was considered significant in this analysis.

Animal studies

Immunocompromised nude mice were obtained from the breeding facility at the animal center of Central South University. All animal studies were performed in accordance with institutional ethical guidelines for experimental animal care. In xenograft study, 1×10^6 Penl2 cells were subcutaneously inoculated into the flank of each nude mice (n = 6). In order to determine tumor volume by external caliper, the greatest longitudinal diameter (a) and the greatest transverse diameter (b) were determined. Tumor volume based on caliper measurements was calculated by the modified ellipsoidal formula: tumor volume (mm^3) = $a \times b^2/2$. Mice were sacrificed 22 days after cell inoculation, and the subcutaneous xenografts were removed, washed by phosphate buffered saline (PBS), and weighted. The expression of *SHCBP1*, p-*STAT3*, *c-Myc*, and Ki-67 in xenograft tissues were evaluated by western blotting and immunohistochemistry.

Statistical analysis

The statistical software package SPSS 16.0 was used in this study. Chi-square test was conducted to analyze the relationship between *SHCBP1* expression and clinicopathological parameters. Kaplan-Meier curves of overall survival were plotted and survival in the groups was compared by log-rank test. Multivariable Cox regression analysis was conducted to identify the prognostic factors that influence overall survival. Significance between two groups was performed using Student's t test. Significance between more than two groups was evaluated by one way analysis of variance (ANOVA). A two-tailed $P < 0.05$ was considered significant in all tests.

Results

SHCBP1 is highly expressed in PC tissues

The mRNA expression of *SHCBP1* in PC was analyzed based on GEO databases (GSE57955). As shown in **Figure 1A**, 87.2% of PC tissues (34/39) exhibited a high level of *SHCBP1* expression (PC vs. normal penile tissue pool (NPT), Log_2 PC/NPT ≥ 2). *SHCBP1* expression did not differ between HPV^+ and HPV^- PC tissues ($P > 0.05$, **Figure 1B**). The expression of *SHCBP1* protein in normal penile tissues (n = 30) and PC tissues (n = 105) was assessed by immunohistochemistry. *SHCBP1* staining was low or absent in normal penile tissues (**Figure 1C**, left panel). Overall, 38.1% (40/105) of PC cases exhibited high *SHCBP1* expression (staining positivity ≥ 30%) (**Figure 1C**, right panel). The association between *SHCBP1* and clinicopathological features of the PC cohort is summarized in **Table 1**. As shown in **Table 1**, high *SHCBP1* expression was significantly related to pathological grade ($P = 0.032$), T stage ($P = 0.017$), lymph node metastasis ($P = 0.003$), and pelvic lymph node metastasis (pelvic LNM) ($P = 0.019$) but not to age ($P = 0.632$), phimosis ($P = 0.965$), body mass index ($P = 0.333$), or histological subtype ($P = 0.266$). Survival analysis showed that high *SHCBP1* expression was associated with shorter overall survival in our PC cohort (**Figure 1D**). We also conducted univariate and multivariate Cox regression analysis, and the results are summarized in **Table 2**. Univariate Cox regression analysis results showed that pathological grade ($P = 0.025$), T stage ($P = 0.006$), nodal status ($P < 0.001$), pelvic LNM ($P < 0.001$), and high *SHCBP1* expression ($P < 0.001$) were prognostic factors for overall survival in our PC cohort (**Table 2**). However, multivariate Cox regression analysis indicated that the nodal status ($P < 0.001$; HR = 8.056), pelvic LNM ($P < 0.001$; HR = 24.437), and high *SHCBP1* expression ($P = 0.025$; HR = 3.106) could serve as independent prognostic

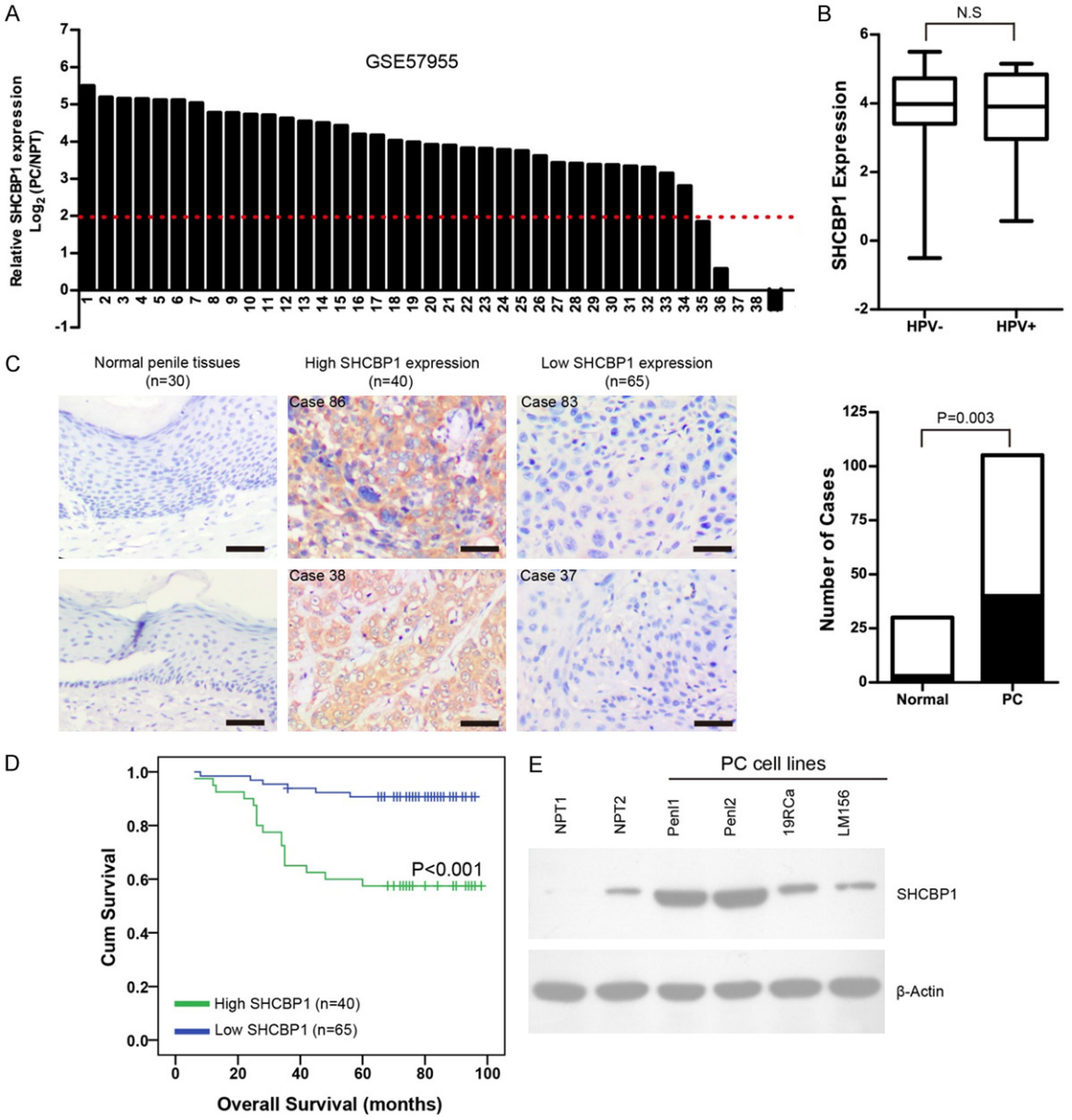

Figure 1. *SHCBP1* is highly expressed in PC and associated with unfavorable prognosis. A. Waterfall plot of relative *SHCBP1* expression in GSE57955 dataset (n = 39). Relative *SHCBP1* expression was calculated with reference to normal penile tissue pool. B. *SHCBP1* expression was not associated with HPV status in GSE57955 dataset. HPV^+ cases vs. HPV^- cases, $P > 0.05$. C. *SHCBP1* was highly expressed in PC tissues (n = 105) compared to normal penile tissues (n = 30). Representing micrographs showed *SHCBP1* expression in normal penile tissues or PC tissues, respectively. Bars: 100 μm. D. High *SHCBP1* expression was associated with unfavorable overall survival in our PC cohort. E. Expression of *SHCBP1* in normal penile tissues (NPT1, NPT2) and a panel of PC cell lines (Penl1, Penl2, LM156, l49RCa). β-Actin was used as loading control.

factors for unfavorable overall survival (**Table 2**). Western blotting showed that *SHCBP1* exhibited differential expression patterns in normal penile tissues (NPT1, NPT2) and a panel of PC cell lines (Penl1, Penl2, 149RCa, and LM156), with high *SHCBP1* expression seen in Penl1 and Penl2 cells (**Figure 1E**).

Knockdown of SHCBP1 expression suppresses malignant phenotypes in SHCBP1-high PC cell lines

We sought to investigate further the oncogenic function of *SHCBP1* in *SHCBP1*-high Penl1 and Penl2 cells. These two cell lines were transfect-

Table 1. Association between clinicopathologic characteristics and SHCBP1 expression in PC cohort

Clinicopathological Parameters	SHCBP1 low expression	SHCBP1 High expression	Odds Ratio	*P* value
Age (year)			1.212	0.632
< 54	34 (53.3%)	19 (47.5%)		
≥ 54	31 (46.7%)	21 (52.5%)		
Phimosis			1.021	0.965
Yes	49 (75.4%)	30 (75.0%)		
No	16 (24.6%)	10 (25.0%)		
Body mass index			1.500	0.333
< 24	45 (69.2%)	24 (60.0%)		
≥ 24	20 (30.8%)	16 (40.0%)		
Pathological grade			2.421	0.032*
G1	46 (70.8%)	20 (45.0%)		
G2 + G3	19 (29.2%)	20 (55.0%)		
Histological subtype			0.609	0.266
Usual	42 (64.6%)	30 (75.0%)		
Others	23 (35.4%)	10 (25.0%)		
T stage			2.667	0.017*
T1	40 (61.5%)	15 (37.5%)		
T2 + T3	25 (38.5%)	25 (62.5%)		
Nodal status			3.451	0.003*
Negative	48 (77.5%)	18 (45.0%)		
Positive	17 (22.5%)	22 (55.0%)		
Pelvic LNM			9.143	0.019*
No	64 (98.5%)	35 (87.5%)		
Yes	1 (1.5%)	5 (12.5%)		

*$P < 0.05$.

Table 2. Univariate and multivariate Cox proportional hazard model for clinicopathological parameters affecting overall survival in PC cohort

Clinicopathological parameters	Univariate analysis		Multivariate analysis	
	HR (95% CI)	*P* value	HR (95% CI)	*P* value
Age (< 54 vs. ≥ 54)		0.266		
Subtype (Usual vs. others)		0.192		
Grade (G2 + G3 vs. G1)	2.613 (1.130-6.043)	0.025		0.062
T stage (T2 + T3 vs. T1)	3.718 (1.465-9.435)	0.006		0.350
Nodal status	6.257 (2.461-15.911)	< 0.001	8.056 (2.760-23.511)	< 0.001
Pelvic LNM	19.821 (7.180-54.715)	< 0.001	24.437 (6.489-92.021)	< 0.001
High SHCBP1 expression	5.633 (2.217-14.311)	< 0.001	3.106 (1.156-8.344)	0.025

ed with non-targeting scrambled (Scr) or specific shRNAs targeting *SHCBP1* (sh-1 and sh-2). As shown in **Figure 2A**, *SHCBP1* expression was greatly reduced by sh*SHCBP1* compared with Scr in Penl1 and Penl2 cells. We next examined the effect of *SHCBP1* expression on the cell growth of PC cells by CCK-8 assay, and the results showed that sh*SHCBP1*-transfected PC cells grew slower than those transfected with Scr shRNA ($P < 0.05$; **Figure 2B**). Caspase-3 activities were increased in *SHCBP1* knockdown groups compared with Scr control groups ($P < 0.05$; **Figure 2C**). Moreover, soft agar clonogenesis of PC cells in sh*SHCBP1* groups decreased greatly, compared with Scr groups ($P < 0.05$; **Figure 2D**). We also observed a sig-

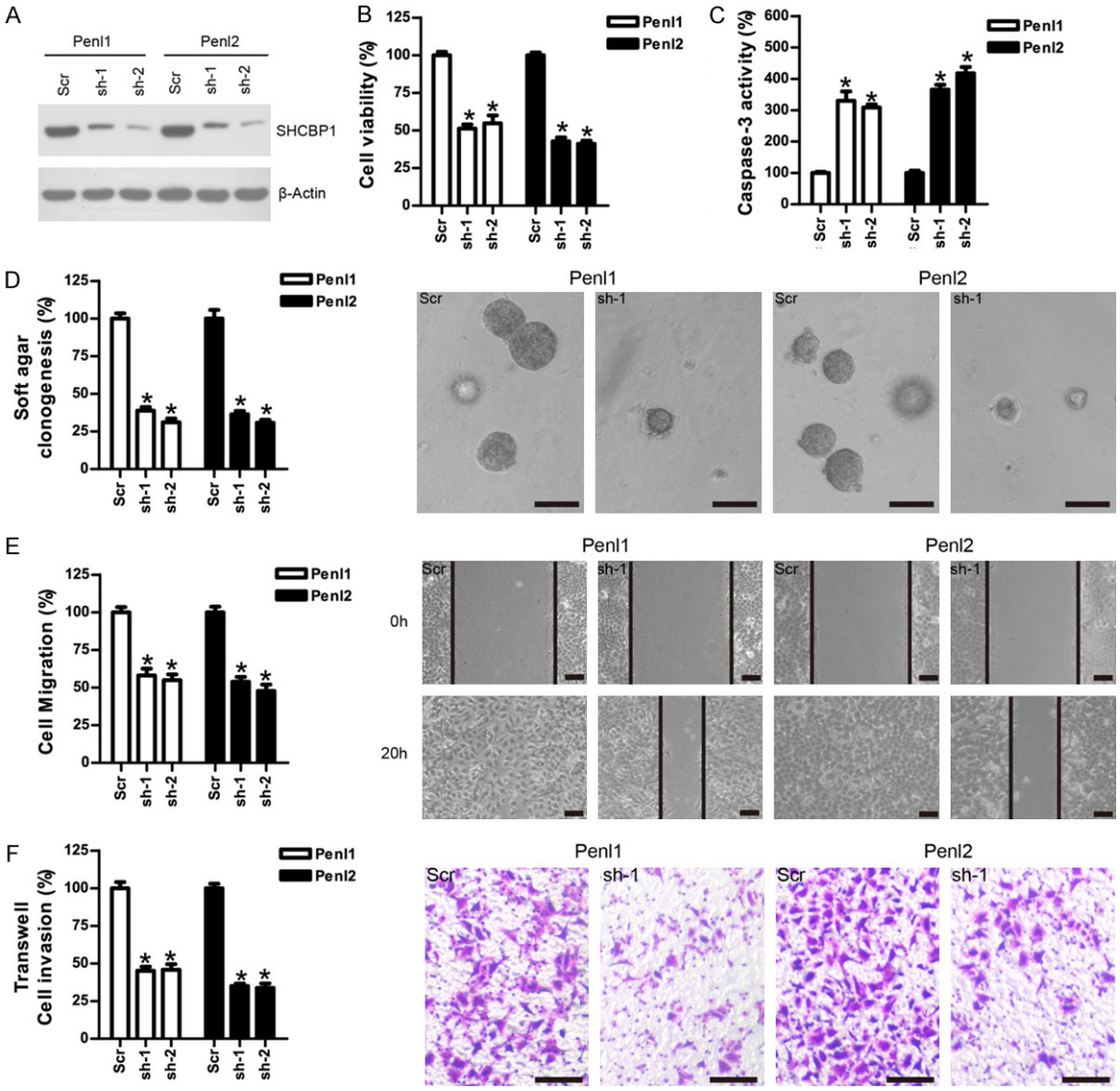

Figure 2. Knockdown of *SHCBP1* impaired the malignant phenotypes in *SHCBP1*-high PC cell lines. A. *SHCBP1* expression was greatly reduced by lentivirus-mediated shRNA knockdown compared to scramble (Scr) control in Penl1 and penl2 cells. β-Actin was used as loading control. B. *SHCBP1* knockdown attenuated cell proliferation in Penl1 and Penl2 cells. The cell viability in Scr control was regards as 100%. n = 4, **P* < 0.05, as compared with Scr control. C. *SHCBP1* knockdown induced caspase-3 activity in Penl1 and Penl2 cells. The caspase-3 activity in Scr control was regards as 100%. n = 3, **P* < 0.05, as compared with Scr control. D. *SHCBP1* knockdown inhibited soft agar clonogenesis in Penl1 and Penl2 cells. The soft agar clonogenesis in Scr control was regards as 100%. n = 3, **P* < 0.05, as compared with Scr control. Bars: 100 μm. E. Knockdown of *SHCBP1* expression inhibited cell migration of PC cells. Bars: 100 μm. The cell migration in Scr control was regards as 100%. n = 3, **P* < 0.05. F. Knockdown of *SHCBP1* expression inhibited transwell invasion of PC cells. Bars: 100 μm. The cell invasion in Scr control was regards as 100%. n = 3, **P* < 0.05.

nificantly retarded wound-healing rate in PC cells expressing sh*SHCBP1* shRNAs compared with those expressing in the Scr control (*P* < 0.05; **Figure 2E**). Transwell invasion assay was also performed to examine the effects of *SHCBP1* on cell invasion. As shown in **Figure 2F**, knockdown of *SHCBP1* expression attenuated the invasion of Penl1 and Penl2 cells compared with Scr control (*P* < 0.05). As both *SHCBP1* shRNAs demonstrated a similar effect on PC cells, *SHCBP1* sh-2 shRNA was used for further experiments. In addition, the cell viability attenuated by *SHCBP1* sh-2 shRNA could be mostly restored by transfection of

recombined shRNA-resistant *SHCBP1* plasmid, suggesting that the off-target effect of sh-2 shRNA might be minimal (Figure S1A, S1B).

Overexpression of SHCBP1 expression promotes malignant phenotypes in SHCBP1-low PC cell lines

The function of *SHCBP1* was also explored in the *SHCBP1*-low PC cell line 149RCa and LM156. As shown in **Figure 3A**, *SHCBP1* expression was significantly increased in 149RCa and LM156 cells transfected with *SHCBP1* lentivirus compared with the empty vector (EV) control. Next, we examined the effect of *SHCBP1* expression on the cell growth of PC cells by CCK-8 assay. *SHCBP1*-expressing PC cells grew faster than those transfected with EV ($P < 0.05$; **Figure 3B**). Caspase-3 activities were decreased in *SHCBP1* groups as compared with that in EV groups ($P < 0.05$; **Figure 3C**). Moreover, soft agar clonogenesis of PC cells in *SHCBP1* groups was significantly increased compared with that in the EV groups ($P < 0.05$; **Figure 3D**). Further, a significantly accelerated wound-healing rate in PC cells expressing *SHCBP1* was observed, compared with those expressing in EV control ($P < 0.05$; **Figure 3E**). Transwell invasion analysis showed that overexpression of *SHCBP1* enhanced the invasion of 149RCa and LM156 cells compared with that in EV control (**Figure 3F**, $P < 0.05$).

SHCBP1 regulates the STAT3/c-Myc signaling pathway in PC cells

A luciferase reporter assay on cancer-related signaling pathways was conducted to identify downstream signaling of *SHCBP1* in PC cells. As shown in **Figure 4A**, knockdown of *SHCBP1* led to a dramatic decline of luciferase reporter activity in *STAT3* and *c-Myc* pathways. A considerable reduction of p-*STAT3* and *c-Myc* levels was observed in *SHCBP1*-depleted Penl1 and Penl2 cells compared with Scr control (**Figure 4B**), whereas overexpression of *SHCBP1* increased p-*STAT3* and *c-Myc* levels in 149RCa and LM156 cells (**Figure 4C**). We conducted RNA sequencing analysis on *SHCBP1*- or *STAT3*-depleted Penl2 cells (Table S1). A number of up-regulated ($Log_2FC \geq 1$, n = 22) and down-regulated ($Log_2FC \leq -1$, n = 99) genes were commonly identified in sh*SHCBP1* and sh*STAT3* group (Figure S2A, S2B). Notably, important genes involved in oncogenic function (*Myc, SOX9, FOXA1, SNAI*), cell cycle regulation (*CCND1, CCNA1, PLK3*), apoptosis (*MCL1, BCL2L1, BAX*), and angiogenesis/inflammation (*VEGFC, IL6, CXCL8, CCL20, IL1A*) were differentially expressed in sh*SHCBP1* and sh*STAT3* group (**Figure 4D**). Pathway and process enrichment analysis showed that the Go biological processes (cytokine-mediated signaling pathway, positive regulation of response to external stimulus, response to virus, regulation of cell death, and cellular response to lipid) and KEGG pathways (transcriptional misregulation in cancer, bladder cancer, IL-17 signaling pathway, AGE-RAGE signaling pathway in diabetic complications, and JAK-STAT signaling pathway) were highly enriched in the down-regulated genes in sh*SHCBP1* and sh*STAT3* group (**Figure 4E**). In contrast, the up-regulated genes were shown to enrich Go biological processes (post-embryonic development, appendage morphogenesis, positive regulation of apoptotic signaling pathway, cellular response to TGF-β stimulus) and KEGG pathways (HTLV-1 infection, pathways in cancer) (**Figure 4E**). Western blotting analysis showed that knockdown of *SHCBP1* or *STAT3* reduced anti-apoptosis genes (*MCL1, BCL-XL*) and induced pro-apoptosis genes (*BAX*, cleaved caspase-3) in Penl1 and Penl2 cells (Figure S2C).

JAK2/STAT3 signaling regulated by SHCBP1 might be driven by EGFR

Immunoprecipitation analysis showed that *SHCBP1* interacts with *STAT3* and its upstream kinase *JAK2* in Penl1 and Penl2 cells (**Figure 5A**). However, the interaction between *JAK2* and *STAT3* was greatly disrupted by *SHCBP1* knockdown in Penl1 and Penl2 cells (**Figure 5B**). *STAT3* is an essential signaling protein engaged by *EGFR* to promote cellular growth, differentiation, and survival in cancer cells [33]. To examine the effect of *EGFR* signaling on *SHCBP1*-regulated *JAK2/STAT3* activation, we treated serum-deprived Penl2 cells with EGF (50 ng/ml) for 6 h. As shown in **Figure 5C**, the interaction between *SHCBP1* and *JAK2*:*STAT3* was considerably induced by EGF. Next, we treated serum-deprived Penl2 cells (Scr or shSHCBP1) with EGF (50 ng/ml) or EGFR inhibitor erlotinib. Western blotting analysis showed that EGF stimulation increased p-*EGFR*, p-*STAT3*, and *c-Myc* expression in *SHCBP1*-expressing

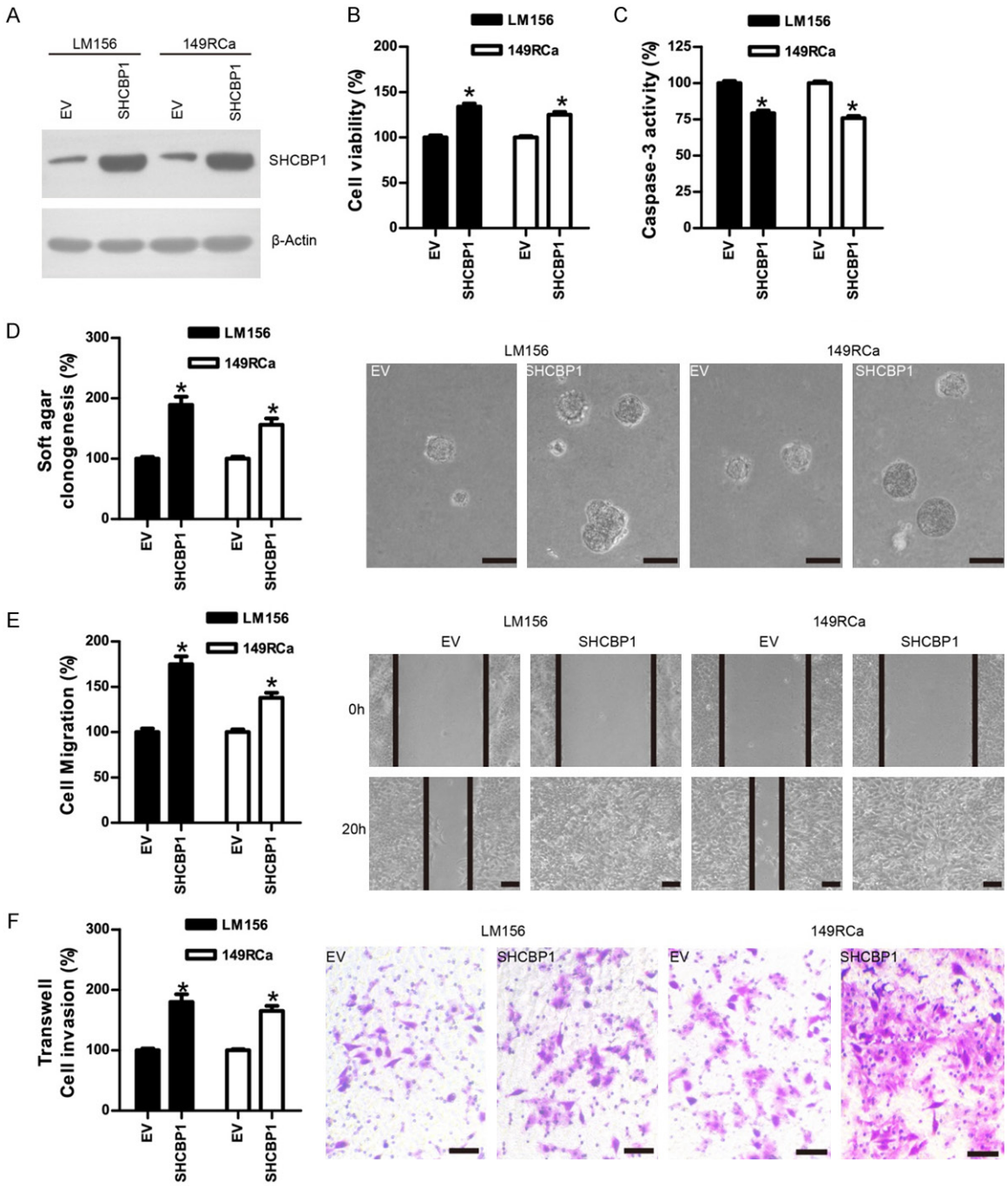

Figure 3. Over-expression of *SHCBP1* enhances the malignant phenotypes in *SHCBP1*-low PC cell lines. A. *SHCBP1* expression was considerably increased by constitutive *SHCBP1* expression compared to empty vector (EV) control in LM156 and 149RCa cells. β-Actin was used as loading control. B. Constitutive *SHCBP1* expression promoted cell proliferation in LM156 and 149RCa cells. The cell viability in EV control was regards as 100%. n = 4, **P* < 0.05, as compared with EV control. C. Over-expression of *SHCBP1* attenuated caspase-3 activity in LM156 and 149RCa cells. The caspase-3 activity in EV control was regards as 100%. n = 3, **P* < 0.05, as compared with EV control. D. Constitutive *SHCBP1* expression enhanced soft agar clonogenesis in LM156 and 149RCa cells. The soft agar clonogenesis in EV control was regards as 100%. n = 3, **P* < 0.05, as compared with EV control. Bars: 100 μm. E. Over-expression of *SHCBP1* expression promoted cell migration of PC cells. Bars: 100 μm. The cell migration in EV control was regards as 100%. n = 3, **P* < 0.05. F. Over-expression of *SHCBP1* enhanced transwell invasion of PC cells. Bars: 50 μm. The cell invasion in EV control was regards as 100%. n = 3, **P* < 0.05.

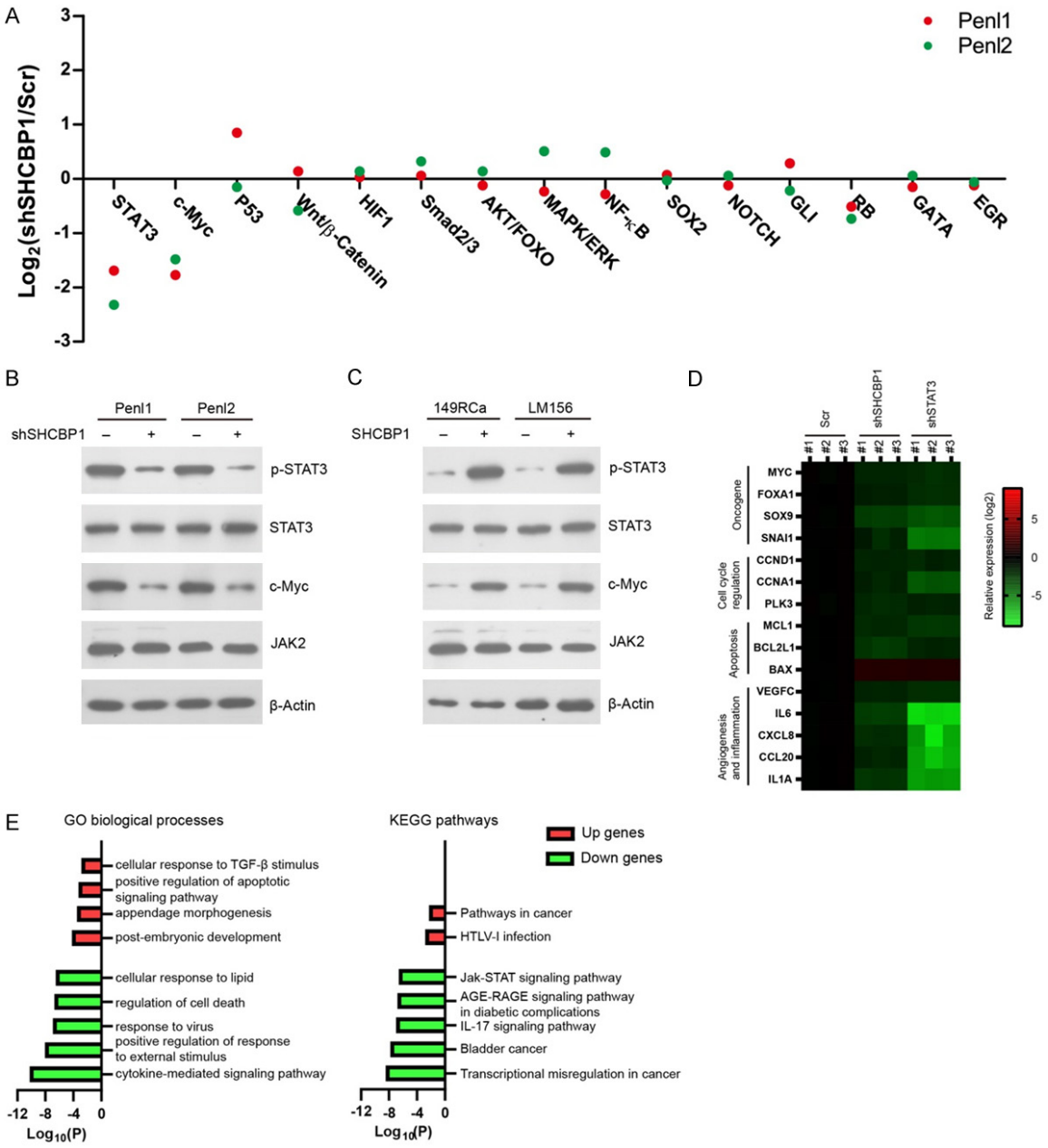

Figure 4. *SHCBP1* regulates downstream *STAT3/c-Myc* signaling in PC cells. A. Multiple pathway reporter analysis identified potential cancer-related pathways regulated by *SHCBP1*. B. Western blotting analysis on *STAT3/c-Myc* signaling following *SHCBP1* depletion in Penl1 and Penl2 cells. C. Western blotting analysis on *STAT3/c-Myc* signaling following over-expression of *SHCBP1* in LM156 and 149RCa cells. D. Heatmap showing differential expression of important genes involved in oncogenic function, cell cycle regulation, apoptosis, and angiogenesis/inflammation in *SHCBP1*- or *STAT3*-depleted Penl2 cells. E. Enrichment of KEGG pathways and GO biological processes in common DEGs in *SHCBP1*- or *STAT3*-depleted Penl2 cells.

Penl2 cells, which was blocked by *EGFR* inhibitor erlotinib; *SHCBP1* depletion led to decreased expression of p-*STAT3* and *c-Myc* in EGF-treated Penl2 cells compared with Scr control (**Figure 5D**). Therefore, the *JAK2/STAT3* signaling regulated by *SHCBP1* might be driven by *EGFR*.

Knockdown of STAT3 or c-Myc attenuates malignant phenotypes in SHCBP1-high PC cell lines

To verify the function of *STAT3/c-Myc* signaling in PC, we depleted *STAT3* or *c-Myc* expression

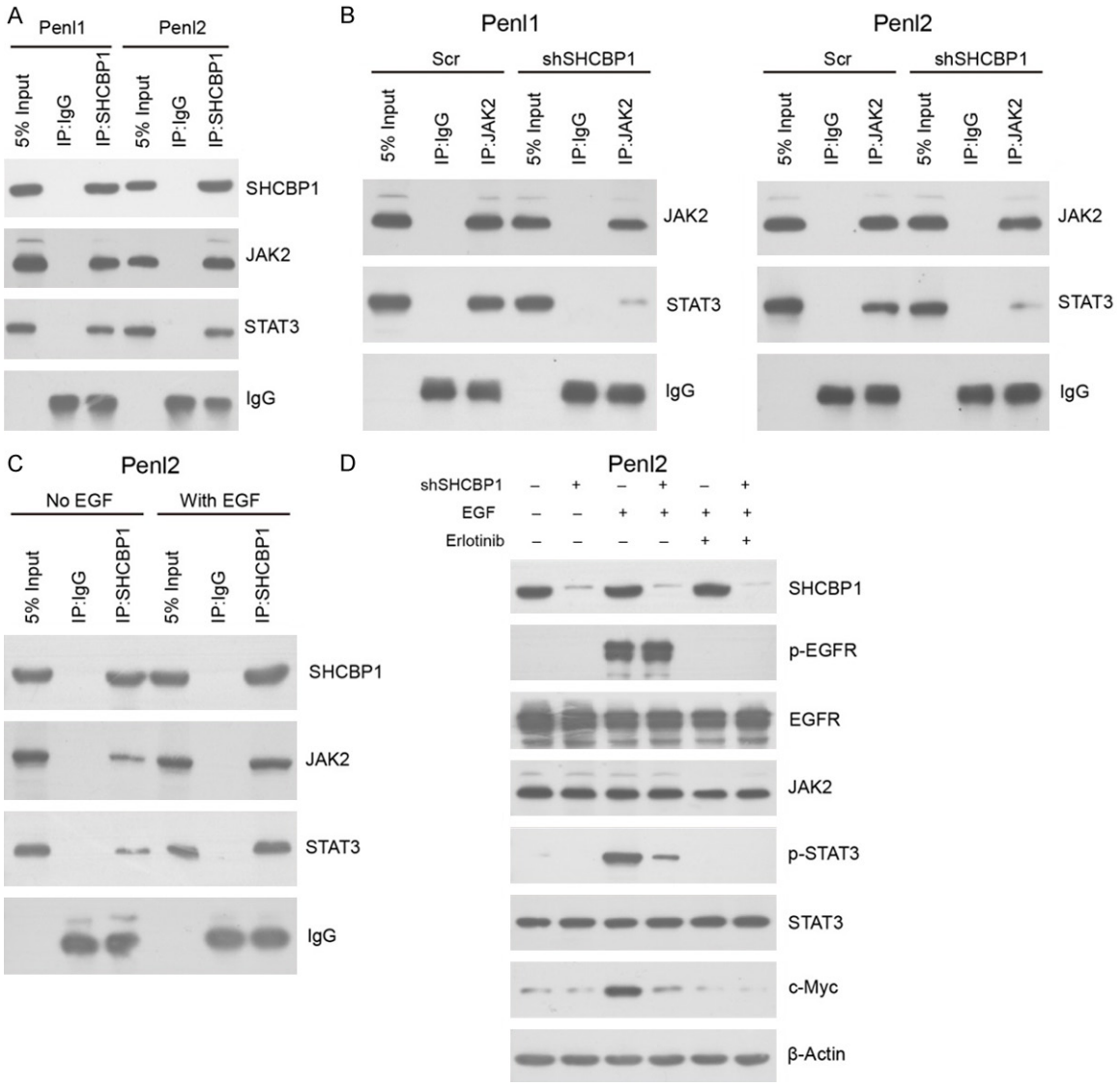

Figure 5. A. *SHCBP1* interacts with *JAK2* and *STAT3* in Penl1 and Penl2 cells. Rabbit anti-*SHCBP1* antibody was used to immunoprecipitate *SHCBP1* protein. Rabbit IgG was used as negative control. B. *SHCBP1* might regulate the interaction between *JAK2* and *STAT3* in Penl1 and Penl2 cells. Rabbit anti-*JAK2* antibody was used to immunoprecipitate *STAT3* proteins. Rabbit IgG was used as negative control. C. *SHCBP1* interacts with *JAK2* and *STAT3* upon EGF stimulation. After serum deprivation for 36 hours, Penl2 cells were stimulated with EGF (50 ng/ml) for 6 hours. *SHCBP1* antibody was used to immunoprecipitate *SHCBP1* protein. Rabbit IgG was used as negative control. D. *SHCBP1* depletion attenuates EGF-induced *STAT3/c-Myc* signaling activation in Penl2 cells. After serum deprivation for 36 hours, PC cells (Scr or sh*SHCBP1*) were stimulated with EGF (50 ng/ml) alone or EGF plus erlotinib (2 μM) for 6 hours. Western blotting was conducted to detect the protein levels of *STAT3/c-Myc* signaling components.

in Penl1 and Penl2 cells (**Figure 6A**). The knockdown *of STAT3* reduced *c-Myc* expression in Penl1 and Penl2 cells, suggesting that *c-Myc* is a downstream target gene of *STAT3* (**Figure 6A**). Next, we examined the cellular function of *STAT3/c-Myc* in Penl1 and Penl2 cells. As shown in **Figure 6B**, sh*STAT3*, or sh*c-Myc*-transfected PC cells grew slower than those transfected with Scr shRNA ($P < 0.05$; **Figure 6B**). Caspase-3 activities were increased in *STAT3* or *c-Myc* knockdown groups compared with that in Scr control groups ($P < 0.05$; **Figure 6C**). Moreover, soft agar clonogenesis of PC cells in the sh*STAT3* or sh*c-Myc* group decreased greatly as compared with that in the Scr group ($P < 0.05$; **Figure 6D**). We also observed a significantly retarded wound-healing rate in PC cells expressing the sh*STAT3* or sh*c-Myc* groups

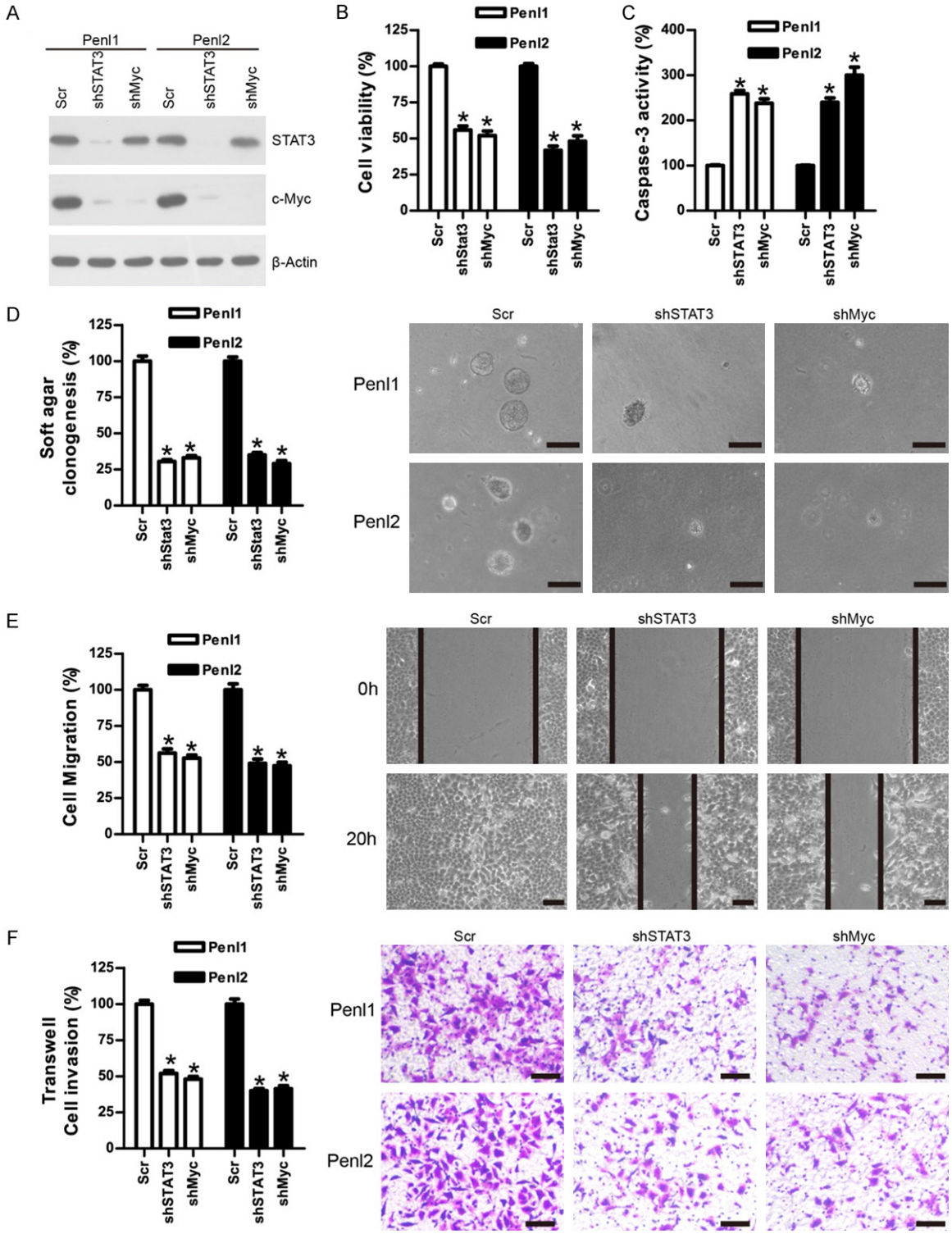

Figure 6. Knockdown of *STAT3* or *c-Myc* impaired the malignant phenotypes in *SHCBP1*-high PC cell lines. A. *STAT3* or *c-Myc* expression was reduced by lentivirus-mediated shRNA knockdown compared to scramble (Scr) control in Penl1 and penl2 cells. β-Actin was used as loading control. B. *STAT3* or *c-Myc* knockdown attenuated cell proliferation in Penl1 and Penl2 cells. The cell viability in Scr control was regards as 100%. n = 4, $*P < 0.05$, as compared with Scr control. C. *STAT3* or *c-Myc* knockdown induced caspase-3 activity in Penl1 and Penl2 cells. The caspase-3 activity in Scr control was regards as 100%. n = 3, $*P < 0.05$, as compared with Scr control. D. *STAT3* or *c-Myc* knockdown inhibited soft agar clonogenesis in Penl1 and Penl2 cells. The soft agar clonogenesis in Scr control was

regards as 100%. n = 3, *P < 0.05, as compared with Scr control. Bars: 100 μm. E. Knockdown of *STAT3* or *c-Myc* expression inhibited cell migration of PC cells. Micrographs showed the results of Penl2 cells. Bars: 100 μm. The cell migration in Scr control was regards as 100%. n = 3, *P < 0.05. F. Knockdown of *STAT3* or *c-Myc* expression inhibited transwell invasion of PC cells. Bars: 50 μm. The cell invasion in Scr control was regards as 100%. n = 3, *P < 0.05.

compared with those expressing in the Scr control (P < 0.05; **Figure 6E**). Transwell invasion assay was also performed to examine the effects of sh*STAT3* or sh*c-Myc* on cell invasion. As shown in **Figure 6F**, knockdown of *STAT3* or *c-Myc* expression attenuated the invasion of Penl1 and Penl2 cells compared with that in Scr control (P < 0.05).

Overexpression of constitutively activated STAT3 or c-Myc partly restores malignant phenotypes in SHCBP1-depleted PC cells

*STAT3*CA (constitutively active), *STAT3*DN (dominant-negative), or *c-Myc* was constitutively expressed in *SHCBP1*-depleted Penl1 and Penl2 cells in order to confirm the hypothesis that *STAT3/c-Myc* signaling is required for *SHCBP1* function in PC. As shown in **Figure 7A**, overexpression of *STAT3CA* or *c-Myc* restored *c-Myc* expression in *SHCBP1*-depleted Penl1 and Penl2 cells. The cellular function of *STAT3* mutants and *c-Myc* was analyzed in Penl1 and Penl2 cells. As shown in **Figure 7B**, in contrast to the empty vector (EV), overexpression of *STAT3CA* or *c-Myc*, but not *STAT3DN*, rescued cell proliferation attenuated by *SHCBP1* knockdown in Penl1 and Penl2 cells. Soft agar clonogenesis of PC cells in the *STAT3*CA or *c-Myc* group was greatly increased compared with that in the EV group (**Figure 7C**). Moreover, caspase-3 activities induced by *SHCBP1* knockdown were markedly reduced by the constitutive expression of *STAT3CA* or *c-Myc* (**Figure 7D**; P < 0.05). The wound-healing rate of PC cells was partly restored in cells expressing *STAT3CA* or *c-Myc* following *SHCBP1* knockdown (**Figure 7E**; P < 0.05). Transwell invasion analysis showed that overexpression of *STAT3CA* or *c-Myc* promoted cellular invasiveness compared with EV in *SHCBP1*-depleted Penl1 and Penl2 cells (**Figure 7F**; P < 0.05).

Knockdown of SHCBP1 attenuates STAT3/c-Myc signaling and suppresses tumor growth in a PC xenograft model

The *in vitro* findings that knockdown of *SHCBP1* suppressed the malignant phenotypes of PC cell lines guided the following in vivo studies. The effect of *SHCBP1* depletion was examined in nude mice with Penl2 subcutaneous xenografts. The group of mice inoculated with Penl2/Scr PC cells grew subcutaneous tumors more rapidly than those with Penl2/sh*SHCBP1* cells (P < 0.05; **Figure 8A**). The tumor weight in the *shSHCBP1* group was significantly smaller than that in the Scr group (**Figure 8B**). Western blotting analysis showed that *SHCBP1* depletion attenuated p-*STAT3* and *c-Myc* expression and induced cleaved caspase-3 in the xenografts (**Figure 8C**). Immunohistochemical staining showed that the sh*SHCBP1* group exhibited decreased *SHCBP1*, p-*STAT3*, *c-Myc*, and Ki-67 expression in the tumors, compared with the Scr control group (**Figure 8D**). Therefore, *SHCBP1* might serve as a potential therapeutic target for PC.

High SHCBP1 expression significantly correlates with STAT3/c-Myc signaling activation in PC

Given the strong effect of *SHCBP1* on PC cell lines, we sought to explore the correlation between *SHCBP1* expression and *STAT3/c-Myc* signaling activation in clinical PC specimens by immunohistochemistry (n = 105). The expression of p-*STAT3* or *c-Myc* was significantly higher in PCs with high *SHCBP1* expression (**Figure 9A**, **9B**), whereas tumors with low *SHCBP1* expression were mostly low for p-*STAT3* or *c-Myc* staining (**Figure 9A**, **9B**). Additionally, GSEA analysis on the GSE57955 dataset confirmed that PC cases with high *SHCBP1* expression (n = 19) also exhibited JAK-*STAT3* signaling pathway activation, as compared with those with low high *SHCBP1* expression (n = 20) (**Figure 9C**). Nevertheless, the correlated expression between *SHCBP1* and *c-Myc* could also be seen in the GSE57955 dataset (**Figure 9D**). Therefore, these data suggested that the *SHCBP1* function might be required for the *STAT3/c-Myc* signaling activation in PC.

Discussion

PC is a rare malignancy for which there are limited treatment options due to a poor understanding of the molecular alterations underly-

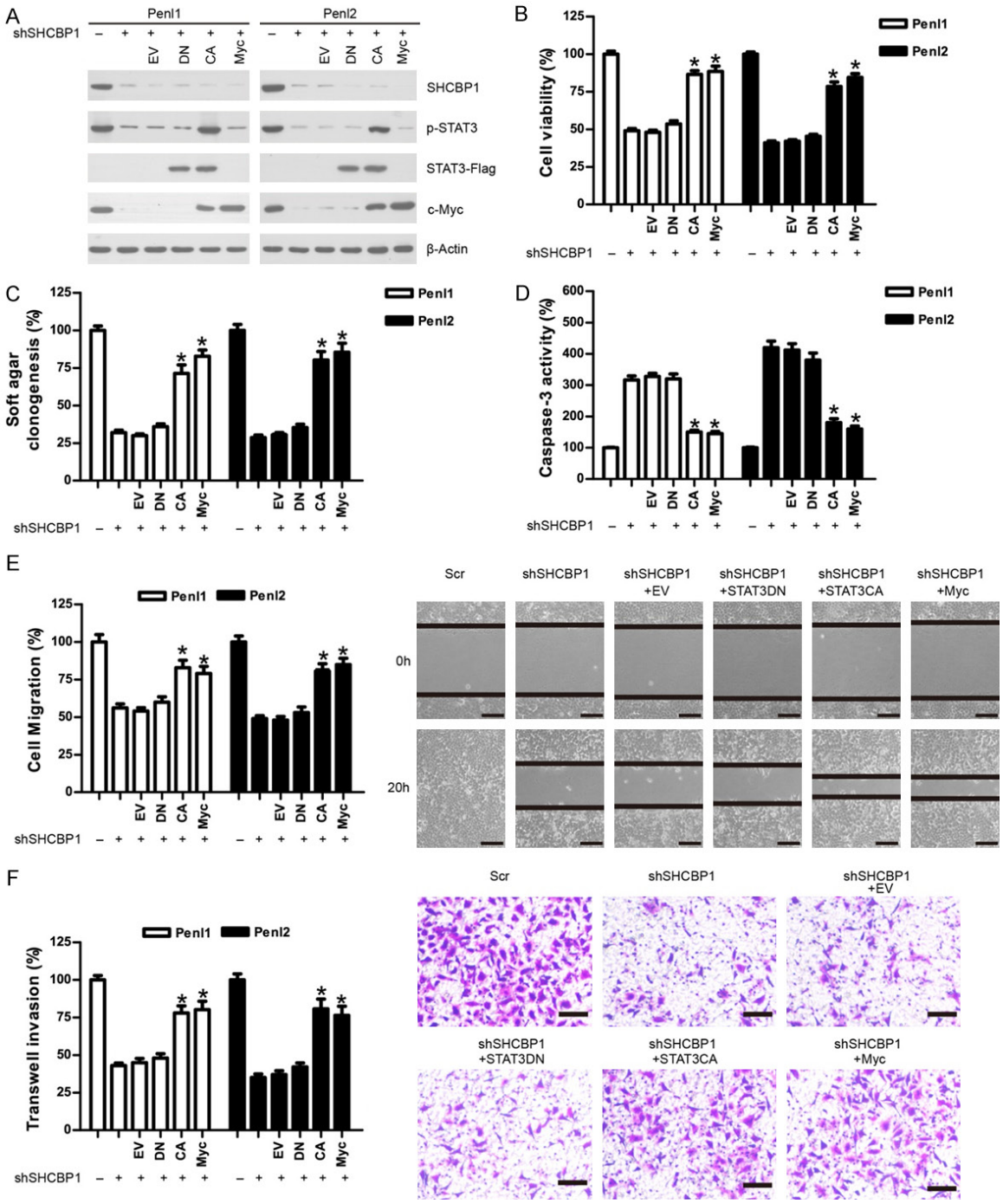

Figure 7. Over-expression of constitutively active *STAT3* or *c-Myc* rescued malignant phenotypes impaired by *SHCBP1* depletion. A. Over-expression of *STAT3*CA (constitutively active), *STAT3*DN (dominant negative) or *c-Myc* in *SHCBP1*-depleted Penl1 and Penl2 cells. B. Over-expression of *STAT3*CA or *c-Myc* rescued cell proliferation suppressed by SHCBP1 depletion. The cell viability in Scr control was regards as 100%. n = 4, $*P < 0.05$, as compared with EV. C. Over-expression of *STAT3*CA or *c-Myc* rescued soft agar clonogenesis inhibited by *SHCBP1* depletion. The soft agar clonogenesis in Scr control was regards as 100%. n = 4, $*P < 0.05$, as compared with EV. D. Over-expression of *STAT3*CA or *c-Myc* reduced caspase-3 activity induced by *SHCBP1* depletion. The caspase-3 activity in Scr control was regards as 100%. n = 3, $*P < 0.05$, as compared with EV. E. Over-expression of *STAT3*CA or *c-Myc* rescued cell migration inhibited by *SHCBP1* depletion. Bars: 100 μm. The cell migration in Scr control was regards as 100%. n =3, $*P < 0.05$, as compared with EV. F. Over-expression of *STAT3CA* or *c-Myc* rescued cell invasion inhibited by *SHCBP1* depletion. Bars: 50 μm. The cell invasion in Scr control was regards as 100%. n = 3, $*P < 0.05$, as compared with EV.

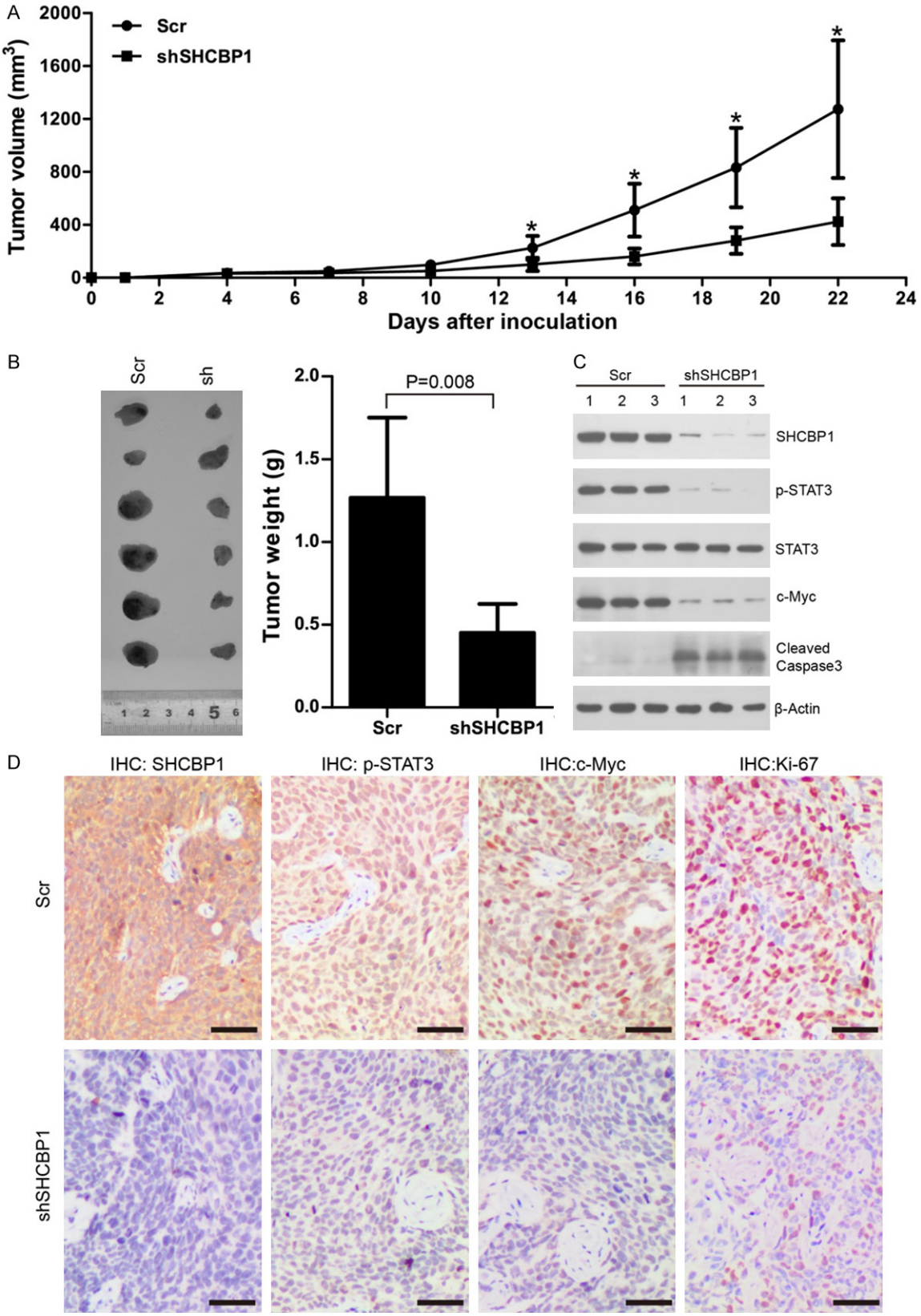

Figure 8. Targeting *SHCBP1* suppressed *in vivo* tumor growth and disrupted *STAT3/c-Myc* signaling. A. *SHCBP1* depletion attenuated subcutaneous xenograft growth. Tumor volume was measured every two days after Penl2 inoculation. n = 6, **P* < 0.05, Scr control vs. sh*SHCBP1*. B. Subcutaneous Penl2 xenografts were taken out at day 22, photographed and weighted. *P* = 0.008, Scr control vs. sh*SHCBP1*. C. Western blotting analysis on protein lysates

extracted from Penl2 xenografts with or without *SHCBP1* depletion. D. Immunohistochemical staining on Penl2 xenografts with or without *SHCBP1* depletion at day 22 after implantation. The tissue sections were incubated with antibodies against indicated antibodies (*SHCBP1*, p-*STAT3*, *c-Myc*, and Ki-67). Diaminobenzidine (DAB) was used as a chromogen, followed by counterstaining with hematoxylin. Bar, 50 μm.

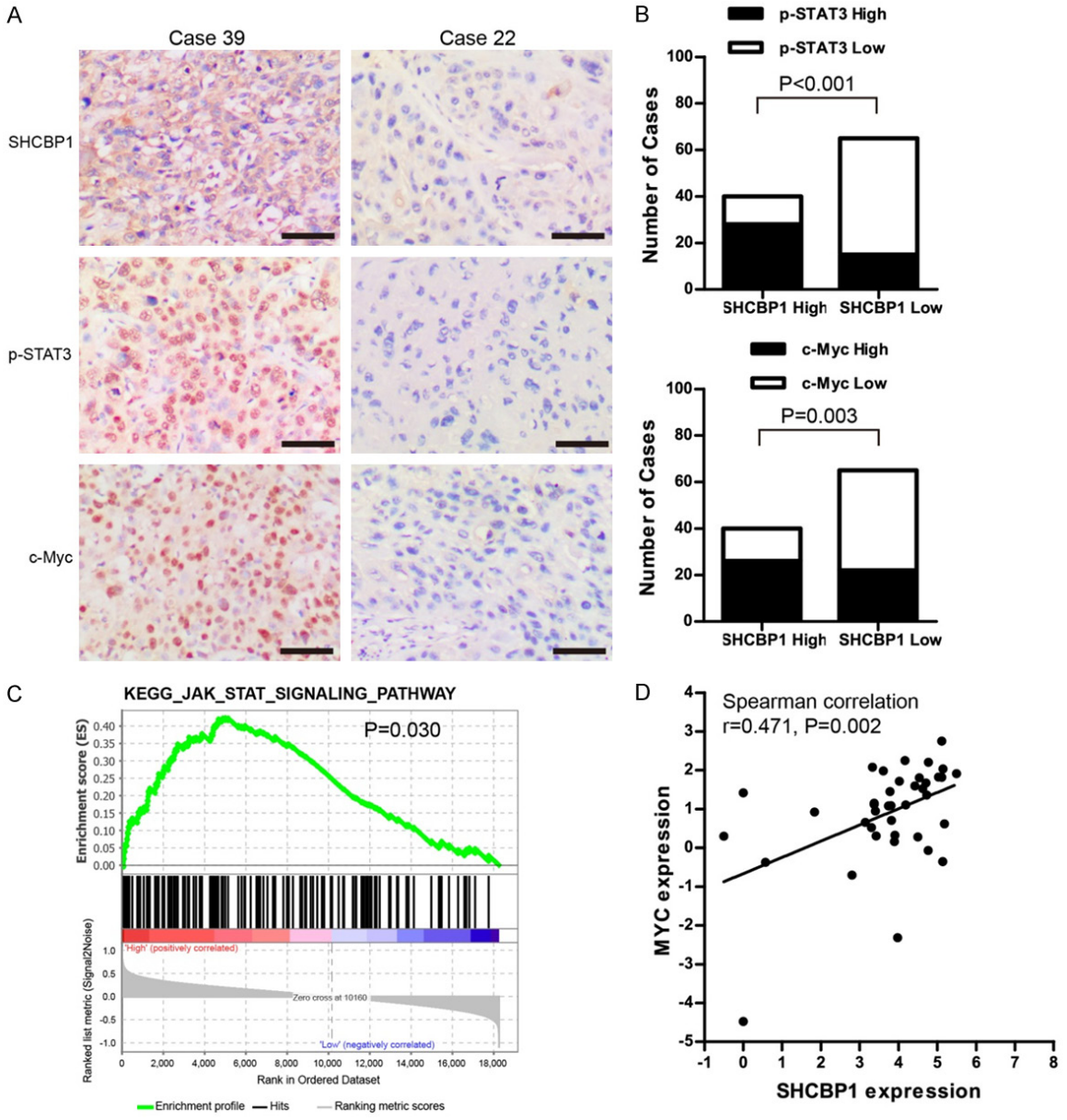

Figure 9. A. Representing micrographs showed consistent expression of *SHCBP1*, p-*STAT3* and *c-Myc* in *SHCBP1*-high or *SHCBP1*-low PC tissues. Bars: 100 μm. B. *SHCBP1* expression was correlated with p-*STAT3* or *c-Myc* in PC samples (n = 105). C. GSEA analysis revealed that *SHCBP1*-high PC cases exhibited highly enriched JAK-*STAT3* signaling in GSE57955 dataset (n = 39). D. The mRNA expression of *SHCBP1* is significantly correlated with *c-Myc* expression in GSE57955 (n = 39).

ing disease development and progression. A better understanding of the molecular alterations involved in PC progression would lead to the identification of molecular markers, providing new targets for therapeutics. Recently, *SHCBP1* was closely associated with cancer development in that aberrant expression of *SHCBP1* has been documented in gastric,

breast, and lung cancer [19, 21, 24]. These findings would implicate *SHCBP1* as a potential oncogene in cancer development.

This study found that *SHCBP1* expression was increased in PC compared with that in normal tissues. Although HPV is a significant contributing factor for approximately 30%-40% of PC, our findings did not reveal the association between *SHCBP1* expression and HPV status, suggesting that the aberrant *SHCBP1* expression in PC might not be caused by HPV infection. Moreover, we showed that *SHCBP1* expression was significantly associated with clinicopathological parameters, including pathological grade, T stage, nodal status, and pelvic LNM, and could serve as an independent prognostic factor for overall survival in PC. Cellular functional analysis showed that the depletion of *SHCBP1* expression suppressed cell proliferation, clonogenesis, and migration/invasion, and induced apoptosis in PC cells. Therefore, these findings suggest that *SHCBP1* serves as a potential cancer marker for PC and exerts important oncogenic function during PC progression.

The function of *SHCBP1* has been proposed to be related to cancer-related signaling pathways, including NF-κB, TGF-β/Smad, and β-catenin. In glioma, *SHCBP1* promotes cell migration and invasion by activating the NF-κB signaling pathway [22]; *SHCBP1* could also promote the metastasis of synovial sarcoma by regulating the TGF-β/Smad signaling pathway [20]. Recently, Liu et al. showed that *SHCBP1* could activate EGF-induced β-Catenin signaling and promote cancer progression in lung cancer cells [34]. Therefore, *SHCBP1* might serve as a crucial mediator that integrates growth factor signaling (TGF-β, EGF) to modulate tumor progression of cancer cells. As *EGFR* is frequently overexpressed in PC and may have an important role in PC carcinogenesis [35-37], it is reasonable to hypothesize that *SHCBP1* might interact with key components of *EGFR* signaling and regulate malignant phenotypes of PC cells.

STAT3 is an essential signaling protein engaged by *EGFR* to promote cellular growth, differentiation, and survival in cancer cells [33, 38]. Recently, *STAT3* was identified as one of the top altered therapeutic targets in PC [39]. In this study, we identified *STAT3/c-Myc* signaling as a potential *SHCBP1* downstream target. The *SHCBP1*:*JAK2*:*STAT3* interaction positively regulates *STAT3* activation and impacts on *c-Myc* expression in PC cells. Furthermore, disruption of *STAT3/c-Myc* signaling attenuated cell proliferation and cell migration/invasion in PC cells, while overexpression of constitutively activated *STAT3* (*STAT3*CA) or *c-Myc* rescued cell proliferation and cell migration/invasion caused by *SHCBP1* depletion in penile cancer cells. Therefore, the *STAT3/c-Myc* pathway might be a crucial downstream signaling of *SHCBP1* in PC. In addition, the difference in downstream signaling activation regulated by *SHCBP1* in PC and other cancer types might reflect the differential requirement of cancer cells to maintain their tumorigenic potential.

The finding that *SHCBP1* regulates cell proliferation and tumorigenesis of PC cells sparked our interest in testing the effect of *SHCBP1* depletion on PC cells in vivo. The effect of *SHCBP1* depletion was confirmed by an in vivo xenograft study in which the transplanted tumors in the *SHCBP1* knockdown group grew slower than those in the Scr control group. Consistent with the *in vitro* findings, *SHCBP1* depletion attenuated *STAT3/c-Myc* signaling and induced apoptosis in the xenograft model. More important, correlated expression of *SHCBP1*, p-*STAT3*, and *c-Myc* was observed in penile cancer tissues, confirming the clinical relevance of *SHCBP1/STAT3/c-Myc* signaling in PC. In conclusion, aberrant *SHCBP1* expression might serve as a potential prognostic biomarker for PC. *SHCBP1* might be a potential oncogene in regulating *STAT3/c-Myc* signaling activation and tumor progression in vitro and in vivo in PC. Our findings highlight the potential significance of *SHCBP1* as a prognostic biomarker and a therapeutic target for PC, which may warrant further investigation in the future.

Acknowledgements

This work was supported by National Nature Science Foundation of China (Grant No. 81902605); Natural Science Foundation of Hunan Province, China (Grant No. 2020JJ5899, 2020JJ5915).

Disclosure of conflict of interest

None.

Address correspondence to: Xiheng Hu, Department of Urology, Xiangya Hospital, Central South University, Changsha 410008, Hunan, China. E-mail: huxiheng@csu.edu.cn

References

[1] Douglawi A and Masterson TA. Updates on the epidemiology and risk factors for penile cancer. Transl Androl Urol 2017; 6: 785-790.

[2] Hu X, Huang J, Wen S, Fu J and Chen M. Comparison of efficacy between brachytherapy and penectomy in patients with penile cancer: a meta-analysis. Oncotarget 2017; 8: 100469-100477.

[3] Teh J, O'Connor E, O'Brien J, Lim WM, Taylor M, Heriot A, Ramsay R and Lawrentschuk N. Future directions in advanced penile cancer - mechanisms of carcinogenesis and a search for targeted therapy. Future Oncol 2020; [Epub ahead of print].

[4] Wen S, Ren W, Xue B, Fan Y, Jiang Y, Zeng C, Li Y and Zu X. Prognostic factors in patients with penile cancer after surgical management. World J Urol 2018; 36: 435-440.

[5] Thomas A, Vanthoor J, Vos G, Tsaur I and Albersen M; collaboration with the European Reference Network for rare urogenital diseases and complex conditions (eUROGEN). Risk factors and molecular characterization of penile cancer: impact on prognosis and potential targets for systemic therapy. Curr Opin Urol 2020; 30: 202-207.

[6] Barski D, Georgas E, Gerullis H and Ecke T. Metastatic penile carcinoma - an update on the current diagnosis and treatment options. Cent European J Urol 2014; 67: 126-132.

[7] Douglawi A and Masterson TA. Penile cancer epidemiology and risk factors: a contemporary review. Curr Opin Urol 2019; 29: 145-149.

[8] Ali SM, Pal SK, Wang K, Palma NA, Sanford E, Bailey M, He J, Elvin JA, Chmielecki J, Squillace R, Dow E, Morosini D, Buell J, Yelensky R, Lipson D, Frampton GM, Howley P, Ross JS, Stephens PJ and Miller VA. Comprehensive genomic profiling of advanced penile carcinoma suggests a high frequency of clinically relevant genomic alterations. Oncologist 2016; 21: 33-39.

[9] Adimonye A, Stankiewicz E, Kudahetti S, Trevisan G, Tinwell B, Corbishley C, Lu YJ, Watkin N and Berney D. Analysis of the PI3K-AKT-mTOR pathway in penile cancer: evaluation of a therapeutically targetable pathway. Oncotarget 2018; 9: 16074-16086.

[10] Arya M, Thrasivoulou C, Henrique R, Millar M, Hamblin R, Davda R, Aare K, Masters JR, Thomson C, Muneer A, Patel HR and Ahmed A. Targets of Wnt/ss-catenin transcription in penile carcinoma. PLoS One 2015; 10: e0124395.

[11] Feber A, Arya M, de Winter P, Saqib M, Nigam R, Malone PR, Tan WS, Rodney S, Lechner M, Freeman A, Jameson C, Muneer A, Beck S and Kelly JD. Epigenetics markers of metastasis and HPV-induced tumorigenesis in penile cancer. Clin Cancer Res 2015; 21: 1196-1206.

[12] Kuasne H, Barros-Filho MC, Busso-Lopes A, Marchi FA, Pinheiro M, Munoz JJ, Scapulatempo-Neto C, Faria EF, Guimaraes GC, Lopes A, Trindade-Filho JC, Domingues MA, Drigo SA and Rogatto SR. Integrative miRNA and mRNA analysis in penile carcinomas reveals markers and pathways with potential clinical impact. Oncotarget 2017; 8: 15294-15306.

[13] Hu X, Chen M, Li Y, Wang Y, Wen S and Jun F. Overexpression of ID1 promotes tumor progression in penile squamous cell carcinoma. Oncol Rep 2019; 41: 1091-1100.

[14] Hu X, Chen M, Li Y, Wang Y, Wen S and Jun F. Aberrant CEACAM19 expression is associated with metastatic phenotype in penile cancer. Cancer Manag Res 2019; 11: 715-725.

[15] Schmandt R, Liu SK and McGlade CJ. Cloning and characterization of mPAL, a novel Shc SH2 domain-binding protein expressed in proliferating cells. Oncogene 1999; 18: 1867-1879.

[16] Asano E, Hasegawa H, Hyodo T, Ito S, Maeda M, Chen D, Takahashi M, Hamaguchi M and Senga T. SHCBP1 is required for midbody organization and cytokinesis completion. Cell Cycle 2014; 13: 2744-2751.

[17] Chen J, Lai F and Niswander L. The ubiquitin ligase mLin41 temporally promotes neural progenitor cell maintenance through FGF signaling. Genes Dev 2012; 26: 803-815.

[18] Buckley MW, Arandjelovic S, Trampont PC, Kim TS, Braciale TJ and Ravichandran KS. Unexpected phenotype of mice lacking Shcbp1, a protein induced during T cell proliferation. PLoS One 2014; 9: e105576.

[19] Dong YD, Yuan YL, Yu HB, Tian GJ and Li DY. SHCBP1 is a novel target and exhibits tumor-promoting effects in gastric cancer. Oncol Rep 2019; 41: 1649-1657.

[20] Peng C, Zhao H, Song Y, Chen W, Wang X, Liu X, Zhang C, Zhao J, Li J, Cheng G, Wu D, Gao C and Wang X. SHCBP1 promotes synovial sarcoma cell metastasis via targeting TGF-beta1/Smad signaling pathway and is associated with poor prognosis. J Exp Clin Cancer Res 2017; 36: 141.

[21] Feng W, Li HC, Xu K, Chen YF, Pan LY, Mei Y, Cai H, Jiang YM, Chen T and Feng DX. SHCBP1 is over-expressed in breast cancer and is important in the proliferation and apoptosis of the human malignant breast cancer cell line. Gene 2016; 587: 91-97.

[22] Zhou Y, Tan Z, Chen K, Wu W, Zhu J, Wu G, Cao L, Zhang X, Zeng X, Li J and Zhang W. Overexpression of SHCBP1 promotes migration and invasion in gliomas by activating the NF-kappaB signaling pathway. Mol Carcinog 2018; 57: 1181-1190.

[23] Xu N, Wu YP, Yin HB, Chen SH, Li XD, Xue XY and Gou X. SHCBP1 promotes tumor cell proliferation, migration, and invasion, and is associated with poor prostate cancer prognosis. J Cancer Res Clin Oncol 2020; 146: 1953-1969.
[24] Zou A, Wu A, Luo M, Zhou C, Lu Y and Yu X. SHCBP1 promotes cisplatin induced apoptosis resistance, migration and invasion through activating Wnt pathway. Life Sci 2019; 235: 116798.
[25] Paner GP, Stadler WM, Hansel DE, Montironi R, Lin DW and Amin MB. Updates in the eighth edition of the tumor-node-metastasis staging classification for urologic cancers. Eur Urol 2018; 73: 560-569.
[26] Zhou QH, Deng CZ, Li ZS, Chen JP, Yao K, Huang KB, Liu TY, Liu ZW, Qin ZK, Zhou FJ, Huang W, Han H and Liu RY. Molecular characterization and integrative genomic analysis of a panel of newly established penile cancer cell lines. Cell Death Dis 2018; 9: 684.
[27] Jun F, Hong J, Liu Q, Guo Y, Liao Y, Huang J, Wen S and Shen L. Epithelial membrane protein 3 regulates TGF-beta signaling activation in CD44-high glioblastoma. Oncotarget 2017; 8: 14343-14358.
[28] Hu X, Chen M, Liu W, Li Y and Fu J. Preoperative plasma IGFBP2 is associated with nodal metastasis in patients with penile squamous cell carcinoma. Urol Oncol 2019; 37: 452-461.
[29] Huber W, Carey VJ, Gentleman R, Anders S, Carlson M, Carvalho BS, Bravo HC, Davis S, Gatto L, Girke T, Gottardo R, Hahne F, Hansen KD, Irizarry RA, Lawrence M, Love MI, MacDonald J, Obenchain V, Oles AK, Pages H, Reyes A, Shannon P, Smyth GK, Tenenbaum D, Waldron L and Morgan M. Orchestrating high-throughput genomic analysis with Bioconductor. Nat Methods 2015; 12: 115-121.
[30] Zhou Y, Zhou B, Pache L, Chang M, Khodabakhshi AH, Tanaseichuk O, Benner C and Chanda SK. Metascape provides a biologist-oriented resource for the analysis of systems-level datasets. Nat Commun 2019; 10: 1523.
[31] Kuasne H, Colus IM, Busso AF, Hernandez-Vargas H, Barros-Filho MC, Marchi FA, Scapulatempo-Neto C, Faria EF, Lopes A, Guimaraes GC, Herceg Z and Rogatto SR. Genome-wide methylation and transcriptome analysis in penile carcinoma: uncovering new molecular markers. Clin Epigenetics 2015; 7: 46.
[32] Subramanian A, Tamayo P, Mootha VK, Mukherjee S, Ebert BL, Gillette MA, Paulovich A, Pomeroy SL, Golub TR, Lander ES and Mesirov JP. Gene set enrichment analysis: a knowledge-based approach for interpreting genome-wide expression profiles. Proc Natl Acad Sci U S A 2005; 102: 15545-15550.
[33] Banerjee K and Resat H. Constitutive activation of STAT3 in breast cancer cells: a review. Int J Cancer 2016; 138: 2570-2578.
[34] Liu L, Yang Y, Liu S, Tao T, Cai J, Wu J, Guan H, Zhu X, He Z, Li J, Song E, Zeng M and Li M. EGF-induced nuclear localization of SHCBP1 activates beta-catenin signaling and promotes cancer progression. Oncogene 2019; 38: 747-764.
[35] Di Lorenzo G, Buonerba C, Ferro M, Calderoni G, Bozza G, Federico P, Tedesco B, Ruggieri V and Aieta M. The epidermal growth factor receptors as biological targets in penile cancer. Expert Opin Biol Ther 2015; 15: 473-476.
[36] Gou HF, Li X, Qiu M, Cheng K, Li LH, Dong H, Chen Y, Tang Y, Gao F, Zhao F, Men HT, Ge J, Su JM, Xu F, Bi F, Gao JJ and Liu JY. Epidermal growth factor receptor (EGFR)-RAS signaling pathway in penile squamous cell carcinoma. PLoS One 2013; 8: e62175.
[37] Chaux A, Munari E, Katz B, Sharma R, Lecksell K, Cubilla AL, Burnett AL and Netto GJ. The epidermal growth factor receptor is frequently overexpressed in penile squamous cell carcinomas: a tissue microarray and digital image analysis study of 112 cases. Hum Pathol 2013; 44: 2690-2695.
[38] Geiger JL, Grandis JR and Bauman JE. The STAT3 pathway as a therapeutic target in head and neck cancer: barriers and innovations. Oral Oncol 2016; 56: 84-92.
[39] Yang ES, Willey CD, Mehta A, Crowley MR, Crossman DK, Chen D, Anderson JC, Naik G, Della Manna DL, Cooper TS and Sonpavde G. Kinase analysis of penile squamous cell carcinoma on multiple platforms to identify potential therapeutic targets. Oncotarget 2017; 8: 21710-21718.

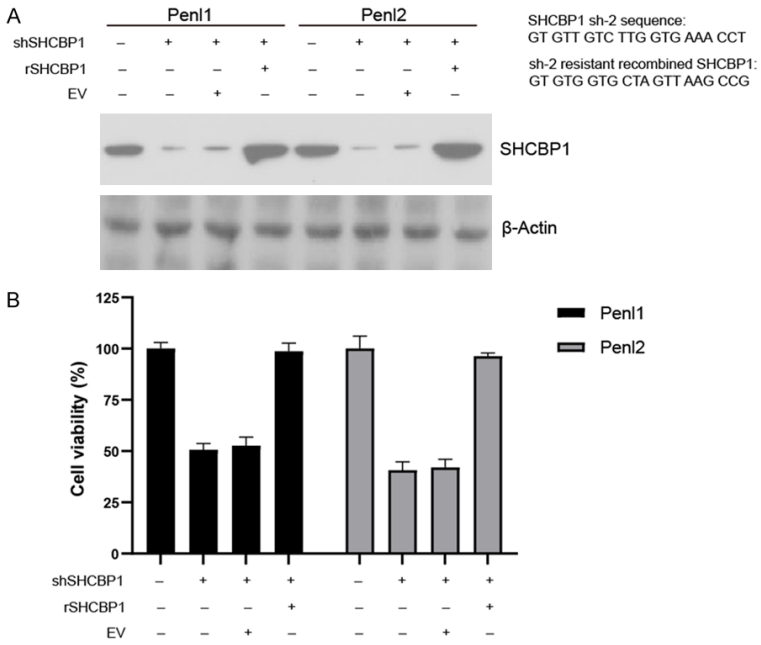

Figure S1. A. Transfection of recombined shRNA-resistant SHCBP1 plasmid restored SHCBP1 expression in SHCBP1-depleted Penl1 and Penl2 cells. B. Transfection of recombined shRNA-resistant SHCBP1 plasmid rescued cell viability attenuated by shSHCBP1 shRNA in Penl1 and Penl2 cells.

Table S1. shSHCBP1 vs. Scr

genesymbol	logFC	*P*.Value	adj.*P*.Val	fold
IGFBP3	3.224872	4.89E-09	4.02E-06	9.349387
TCN1	-3.01818	1.44E-05	0.000325	0.123435
PDP2	-2.89304	0.014429	0.039691	0.134619
IGF2BP3	-2.4053	3.02E-06	0.00011	0.18877
S100P	-2.37095	1.40E-07	1.69E-05	0.193318
ZBTB32	-2.36947	2.53E-06	9.86E-05	0.193516
RASD1	-2.33833	1.64E-10	1.65E-06	0.197739
AIF1L	-2.28782	3.13E-07	2.64E-05	0.204785
SYT7	2.229504	4.17E-10	2.09E-06	4.689727
CXCL2	-2.13705	2.75E-08	7.09E-06	0.227345
TMEM97	-2.12148	5.47E-08	9.64E-06	0.229811
SOX9	-2.11982	2.07E-09	2.98E-06	0.230076
ZDHHC20	-2.11208	5.11E-06	0.000158	0.231314
IL6	-2.10334	3.32E-09	3.71E-06	0.232718
MPZL1	-2.10238	1.47E-09	2.96E-06	0.232874
CDRT4	-2.09677	0.010624	0.031502	0.233782
CA9	2.089698	1.79E-07	1.91E-05	4.256591
UGT1A5	-2.07479	1.84E-09	2.98E-06	0.237369
ANKRD22	-2.02976	7.15E-10	2.39E-06	0.244896
FLI1	-2.00615	1.11E-08	5.19E-06	0.248936
PTGER4	-1.95619	0.000202	0.001903	0.257708
CREB3L3	-1.95606	0.000199	0.001883	0.257731
BCL2L1	-1.93936	8.02E-09	4.74E-06	0.260732
IGFBP2	1.937191	4.73E-09	4.02E-06	3.829593

DAG1	-1.88672	0.04024	0.084678	0.270422
SAR1A	-1.85776	1.27E-09	2.96E-06	0.275905
SPP1	-1.85018	6.07E-06	0.00018	0.277358
HMGCS1	-1.79526	4.46E-06	0.000144	0.28812
IL1A	-1.79244	3.88E-09	3.89E-06	0.288683
INSIG1	-1.78836	1.35E-05	0.00031	0.2895
SHCBP1	-1.75277	7.12E-08	1.12E-05	0.296731
SLC47A1	-1.74599	9.21E-07	5.05E-05	0.298129
S100A9	-1.74261	5.69E-06	0.000172	0.298828
WDR6	1.731686	1.97E-05	0.000407	3.321156
KIF21B	-1.71887	7.98E-09	4.74E-06	0.303787
STK4	1.718612	5.21E-09	4.02E-06	3.291197
NT5E	-1.71277	2.65E-09	3.33E-06	0.305074
LGALS7B	1.696715	2.63E-08	7.09E-06	3.241619
RAB31	-1.6877	0.01785	0.046304	0.310422
PI3	-1.66489	6.83E-08	1.12E-05	0.315368
USH1G	1.654651	1.19E-08	5.19E-06	3.148471
RSAD2	-1.61838	7.11E-09	4.74E-06	0.3257
TMEM171	-1.61757	2.22E-07	2.17E-05	0.325883
RRAD	-1.61223	7.60E-06	0.000211	0.327093
KRT14	1.600956	1.04E-08	5.19E-06	3.033443
SLC25A43	1.588536	9.19E-05	0.001117	3.00744
SPRY4	-1.58538	2.02E-06	8.44E-05	0.333237
IL7R	-1.58271	1.59E-08	6.13E-06	0.333855
HES2	1.581992	0.033197	0.07333	2.99383
CHST11	1.58088	0.023722	0.057454	2.991523
GDF15	-1.56505	1.71E-08	6.36E-06	0.337965
PTN	1.558355	1.03E-05	0.000255	2.945178
HBEGF	-1.55309	2.31E-08	6.93E-06	0.340778
OLFML2A	1.547612	7.34E-09	4.74E-06	2.923329
MED29	1.531398	0.015772	0.042322	2.890658
DUSP4	-1.50886	1.09E-08	5.19E-06	0.35139
C11orf86	-1.49936	0.000119	0.001325	0.35371
CPE	1.49351	2.22E-08	6.93E-06	2.815732
LOX	1.492751	3.59E-08	8.25E-06	2.814251
CXCL8	-1.49165	6.35E-08	1.08E-05	0.355605
EDN2	1.478594	1.60E-07	1.81E-05	2.78677
CHAC1	-1.47588	2.74E-08	7.09E-06	0.359515
TEAD1	-1.47479	0.026978	0.063176	0.359785
SYNGR2	-1.4722	1.89E-07	1.99E-05	0.360432
NRP2	-1.46548	1.14E-08	5.19E-06	0.362115
SOX7	-1.46399	1.11E-08	5.19E-06	0.36249
SOCS3	-1.45794	5.41E-07	3.54E-05	0.364011
ARL8B	1.45774	0.040835	0.085679	2.746777
TEN1	1.449265	0.006023	0.020652	2.730689
TMEM45A	1.44435	4.41E-08	8.36E-06	2.721402
DBI	-1.44383	1.43E-08	5.97E-06	0.367589
YTHDF3	-1.44383	1.42E-05	0.00032	0.36759

CIPC	1.443721	0.022153	0.054669	2.720215
TREX1	-1.43968	0.007425	0.024037	0.368648
RNF4	1.438366	1.55E-06	7.15E-05	2.710138
HGSNAT	1.425613	0.000643	0.004314	2.686286
F3	-1.42532	2.27E-08	6.93E-06	0.372336
NREP	1.424556	0.00027	0.002331	2.684319
PLK3	-1.41256	3.48E-07	2.79E-05	0.375645
MSMO1	-1.40828	2.96E-08	7.43E-06	0.376761
LDLR	-1.40558	1.19E-07	1.57E-05	0.377466
MDFIC	-1.40502	0.016636	0.043948	0.377613
MCL1	-1.40182	2.62E-08	7.09E-06	0.378451
ANG	1.401264	2.30E-08	6.93E-06	2.641328
ADGRA2	1.398909	0.000187	0.0018	2.63702
ZBED6CL	-1.39631	2.10E-08	6.93E-06	0.379899
MT1X	1.39488	5.61E-08	9.72E-06	2.629667
TGIF2	1.390097	0.010409	0.031013	2.620962
LMO1	1.373171	8.17E-07	4.86E-05	2.590393
SYCE2	1.368621	1.56E-08	6.13E-06	2.582237
ETV1	-1.36769	4.11E-08	8.25E-06	0.38751
NECAP1	-1.36596	1.16E-07	1.56E-05	0.387975
FSTL1	1.36491	1.05E-07	1.45E-05	2.575603
DUSP6	-1.36371	1.42E-07	1.69E-05	0.388583
MRAP2	1.360636	8.93E-06	0.000229	2.567983
ACTN1	-1.35968	9.72E-07	5.18E-05	0.389669
PDF	-1.35702	7.91E-05	0.001009	0.390389
GNPNAT1	-1.35139	9.29E-05	0.001125	0.391914
NDRG1	1.350309	1.88E-08	6.75E-06	2.549667
NUPR1	1.34833	9.23E-08	1.32E-05	2.546172
UBFD1	-1.34273	0.011385	0.033145	0.394273
IDI1	-1.34246	2.46E-08	7.07E-06	0.394346
GPR68	1.337939	7.06E-08	1.12E-05	2.527899
MAFG	-1.33341	4.39E-08	8.36E-06	0.396828
KRT13	1.328113	3.80E-08	8.25E-06	2.510741
OASL	-1.32202	2.35E-08	6.93E-06	0.399976
SC5D	-1.31043	0.004364	0.016411	0.403199
RNASE4	1.308109	0.000106	0.001227	2.476167
STS	-1.3066	1.64E-07	1.81E-05	0.404272
MYH14	1.304819	1.53E-07	1.78E-05	2.470527
ERI1	-1.29851	0.000344	0.002785	0.406545
FOSL1	-1.29654	8.05E-08	1.23E-05	0.407103
EREG	-1.29586	1.75E-06	7.76E-05	0.407293
RIMKLB	-1.29538	1.31E-07	1.65E-05	0.40743
SLC35E1	-1.29156	3.45E-07	2.79E-05	0.40851
LIF	-1.29139	3.96E-08	8.25E-06	0.408556
C3	-1.28516	3.09E-08	7.51E-06	0.410324
PDPN	1.27943	9.30E-07	5.07E-05	2.42743
DDAH1	-1.27866	4.27E-08	8.36E-06	0.412179
NR4A2	-1.27864	2.62E-05	0.000493	0.412184

AASDHPPT	-1.27825	1.47E-07	1.73E-05	0.412296
IL20RB	1.278095	3.99E-08	8.25E-06	2.425185
DUSP5	-1.2761	3.14E-08	7.51E-06	0.41291
MMP13	1.274226	3.78E-08	8.25E-06	2.41869
CCL20	-1.27393	1.36E-07	1.68E-05	0.41353
TGM2	-1.26978	3.75E-08	8.25E-06	0.414723
ETV5	-1.26907	7.06E-08	1.12E-05	0.414927
FDFT1	-1.26689	8.77E-08	1.29E-05	0.415555
MYC	-1.25845	6.34E-07	4.00E-05	0.417993
MEGF9	1.258043	4.10E-08	8.25E-06	2.391711
PYROXD1	-1.25488	0.000126	0.001366	0.419028
ARF4	-1.25423	0.000796	0.005028	0.419217
CCND1	-1.25025	5.44E-08	9.64E-06	0.420375
ORAI3	1.249263	0.023755	0.057492	2.377199
PET117	-1.24839	3.91E-07	3.01E-05	0.420917
HIST2H2AC	-1.24545	0.000386	0.00303	0.421777
MEGF6	1.243878	5.72E-06	0.000172	2.368343
GPD1L	1.238479	0.013222	0.0371	2.359496
VEGFC	-1.23306	4.57E-08	8.50E-06	0.425413
TIAF1	-1.22547	0.023555	0.057147	0.427659
CCL24	-1.22477	0.002377	0.010699	0.427867
SNAI1	-1.22467	4.63E-05	0.000714	0.427896
STRADB	-1.22438	8.18E-07	4.86E-05	0.427982
LAPTM5	-1.22317	3.71E-07	2.89E-05	0.428342
BAX	1.221884	4.89E-08	8.92E-06	2.332511
TMEM251	-1.2193	0.008497	0.026653	0.429491
SEMA7A	-1.21897	9.04E-07	5.02E-05	0.429588
WNT10A	1.214753	1.16E-07	1.56E-05	2.321011
ZNF791	1.199638	0.039665	0.083789	2.29682
CCNA1	-1.1974	9.75E-07	5.18E-05	0.43606
JMJD7	-1.19711	0.006852	0.022721	0.436147
BMF	1.197094	1.29E-07	1.65E-05	2.292773
CCL5	-1.19628	0.000605	0.004145	0.436398
TTF1	-1.19508	9.99E-07	5.28E-05	0.436761
LCN2	-1.19151	1.35E-05	0.00031	0.437844
FTO	-1.18747	1.64E-07	1.81E-05	0.439073
RCC1	-1.18709	7.44E-08	1.15E-05	0.439188
CRISPLD2	-1.18495	0.002248	0.010276	0.439839
UNKL	-1.18396	8.78E-06	0.000227	0.440143
HILPDA	1.183744	9.06E-05	0.001106	2.271655
KIAA1191	-1.18231	9.77E-08	1.38E-05	0.440646
PLEKHA2	-1.18119	0.002078	0.009733	0.440989
KLHDC8B	1.17941	4.47E-06	0.000144	2.264842
FAM107B	-1.1762	1.66E-07	1.81E-05	0.442516
CA12	1.171299	0.000287	0.002435	2.252144
NEFL	1.163464	3.93E-07	3.01E-05	2.239946
FIBCD1	1.153553	2.73E-06	0.000104	2.224611
STAMBPL1	-1.15195	2.36E-07	2.19E-05	0.450015

NMI	-1.15098	6.89E-08	1.12E-05	0.45032
GSTA4	1.150174	6.52E-05	0.000894	2.219406
ZBED1	-1.14919	0.01405	0.038898	0.450879
HEATR1	-1.14797	8.51E-08	1.28E-05	0.451259
ENO2	1.14779	9.07E-08	1.32E-05	2.215741
ZNF707	-1.14407	3.10E-05	0.000541	0.45248
HLA-C	1.14363	0.005972	0.020542	2.209362
CLDN4	-1.1412	0.004527	0.016823	0.453383
TNFAIP2	-1.13901	0.000449	0.003342	0.454071
LIMS1	-1.12921	0.000324	0.002663	0.457167
TMC4	1.124352	2.24E-07	2.17E-05	2.180036
CCNJ	-1.12365	3.92E-05	0.00063	0.458933
LRRC61	-1.11862	6.39E-07	4.01E-05	0.460535
B3GNT5	-1.11683	0.002704	0.011632	0.461105
SLC7A8	1.116561	1.15E-06	5.80E-05	2.168296
DIO2	-1.11525	2.37E-07	2.19E-05	0.461612
PIM2	-1.10607	9.86E-08	1.38E-05	0.464557
GRPEL2	-1.10284	0.033208	0.073338	0.465598
EDIL3	1.101517	1.26E-07	1.62E-05	2.145803
MIER1	-1.1003	1.76E-07	1.90E-05	0.466418
LGALS7	1.097872	0.00016	0.001625	2.140388
SELENOP	1.097409	1.37E-06	6.63E-05	2.1397
SKA1	-1.09457	2.99E-06	0.00011	0.468275
ETV4	-1.09118	9.02E-07	5.02E-05	0.469377
FAM83E	-1.08933	7.18E-06	0.000204	0.469978
UMAD1	-1.08677	0.001546	0.007974	0.470814
GNE	-1.08508	1.38E-07	1.69E-05	0.471367
FAM229B	1.084522	2.93E-05	0.000524	2.120673
ORMDL3	-1.08377	0.013883	0.038572	0.471793
ADARB1	-1.08243	7.52E-07	4.64E-05	0.472232
PEX10	1.080818	2.13E-07	2.12E-05	2.115235
FOXO6	1.080097	2.14E-06	8.90E-05	2.114178
SEZ6L2	1.078637	8.28E-07	4.89E-05	2.11204
NFKBIZ	-1.07689	2.58E-05	0.00049	0.474048
IFIT2	-1.07542	1.26E-07	1.62E-05	0.474534
THBD	-1.07411	2.05E-07	2.05E-05	0.474963
SPRR1B	1.07359	2.67E-05	0.000498	2.104664
NFAT5	-1.07276	0.040739	0.085514	0.475408
EGR2	-1.07227	0.000203	0.001911	0.475569
FOXA1	-1.07087	2.80E-07	2.46E-05	0.476033
PCMTD1	-1.06981	0.000386	0.00303	0.476382
ARHGDIB	-1.06973	1.63E-07	1.81E-05	0.476407
CYP1B1	1.061012	4.06E-07	3.04E-05	2.086395
COL5A1	1.060484	1.64E-07	1.81E-05	2.085631
HERC5	-1.06036	4.54E-07	3.24E-05	0.479511
PEG10	-1.05787	0.030705	0.069365	0.480342
SAMD11	1.056853	4.83E-07	3.34E-05	2.080389
CBX1	1.055777	0.016443	0.043615	2.078837

HBB	-1.05403	0.004187	0.015928	0.481623
NRG1	-1.05302	2.81E-07	2.46E-05	0.481957
EPHA2	-1.05108	1.92E-07	1.99E-05	0.482608
ZMYND11	-1.05104	0.00032	0.002637	0.482621
SHISA2	-1.04969	5.00E-05	0.000756	0.483073
UBE2V1	1.047423	0.031213	0.070198	2.066835
ACER3	-1.04551	0.009504	0.029051	0.484474
SEMA3C	1.04416	2.45E-07	2.19E-05	2.062165
TMEM189	-1.0429	2.13E-05	0.00043	0.485351
PMEPA1	1.042361	2.59E-06	0.000101	2.059595
ARHGAP23	-1.03947	0.000924	0.005563	0.486508
PSMG1	-1.03698	3.09E-07	2.63E-05	0.487345
FGFBP1	-1.03615	2.25E-07	2.17E-05	0.487628
CCDC137	-1.03601	0.026114	0.061574	0.487674
C17orf80	1.035251	0.001117	0.006279	2.049471
RCN3	1.033823	2.37E-06	9.36E-05	2.047442
MMP1	-1.03376	3.53E-07	2.82E-05	0.488437
TACSTD2	-1.03232	2.40E-07	2.19E-05	0.488925
EHF	-1.03174	7.90E-07	4.78E-05	0.489119
POLM	-1.03128	0.003307	0.013392	0.489276
THBS1	-1.03046	2.39E-07	2.19E-05	0.489555
AKAP2	-1.02911	0.000297	0.002497	0.490012
GAS1	1.026741	1.37E-05	0.000313	2.037417
NUTF2	-1.0249	4.78E-07	3.34E-05	0.491444
CLCA2	1.023995	4.25E-07	3.10E-05	2.033542
JADE2	-1.02331	2.39E-07	2.19E-05	0.491985
ANKRD2	-1.02303	0.000438	0.003291	0.49208
PCYT2	-1.02179	3.96E-07	3.01E-05	0.492505
SNX15	1.021644	5.00E-07	3.37E-05	2.030231
DKK1	-1.02046	3.32E-07	2.73E-05	0.492958
IFIT3	-1.02	2.90E-07	2.51E-05	0.493116
TMED2	-1.01912	1.92E-07	1.99E-05	0.493418
SYTL3	-1.01745	3.25E-07	2.72E-05	0.493989
TRAPPC6B	-1.01733	1.43E-06	6.78E-05	0.494028
COL7A1	1.016618	2.29E-07	2.19E-05	2.02317
IER5	-1.01607	2.01E-07	2.03E-05	0.494461
ISG15	-1.01529	1.50E-06	7.04E-05	0.49473
BTN3A2	1.014963	0.004673	0.017245	2.02085
GPAM	-1.01264	1.97E-07	2.02E-05	0.495639
TMEM185A	1.012188	2.26E-06	9.16E-05	2.016967
TSPAN17	1.011845	3.32E-06	0.000116	2.016488
KRT16	1.010402	7.17E-07	4.46E-05	2.014473
SLC1A4	1.007193	4.83E-07	3.34E-05	2.009996
ARRDC3	1.007166	3.08E-07	2.63E-05	2.009959
SLC35A5	1.006812	7.73E-07	4.71E-05	2.009466
PSCA	-1.00638	2.42E-07	2.19E-05	0.497793
MMACHC	-1.00475	1.94E-06	8.26E-05	0.498356
ZFP36	-1.00455	2.47E-05	0.000479	0.498425

ISG20	-1.00433	7.86E-06	0.000215	0.498503
SLC6A6	1.00346	0.031813	0.071229	2.004802
SELENON	1.000589	0.012911	0.036354	2.000816
GNG10	-10.8157	6.94E-19	7.73E-16	0.000555
EGR2	-9.82226	2.67E-17	1.14E-14	0.001105
RPS10	-9.79767	1.80E-19	4.52E-16	0.001124
FMC1	-9.79417	5.93E-15	5.12E-13	0.001126
G0S2	-9.75548	2.76E-20	2.76E-16	0.001157
AP3S2	-8.86793	2.23E-15	2.52E-13	0.00214
NBL1	-8.67267	1.17E-12	2.92E-11	0.002451
CSNK1E	-8.63552	1.14E-09	5.70E-09	0.002514
CCND2	-8.57186	6.21E-20	3.12E-16	0.002628
ANKHD1-EIF4EBP3	-8.56867	4.92E-17	1.83E-14	0.002634
RPP21	-8.39983	4.37E-10	2.60E-09	0.002961
GNE	-8.26094	1.08E-10	8.62E-10	0.00326
ST20-MTHFS	-8.22054	3.95E-15	3.69E-13	0.003353
EGR3	-8.20093	1.08E-16	2.84E-14	0.003398
HIST2H2AA4	-8.11748	1.23E-09	6.07E-09	0.003601
EGR1	-7.99324	2.90E-19	5.81E-16	0.003925
ZNF750	-7.99232	1.29E-18	1.30E-15	0.003927
MRPS24	-7.89787	5.85E-18	3.91E-15	0.004193
SGK3	-7.8791	1.73E-19	4.52E-16	0.004248
FAM25A	-7.60801	6.96E-17	2.14E-14	0.005126
CTGF	-7.60406	5.34E-19	6.92E-16	0.00514
UGT1A4	-7.54152	4.86E-09	1.91E-08	0.005368
FOS	-7.48095	5.52E-19	6.92E-16	0.005598
IL6	-7.46796	6.62E-17	2.14E-14	0.005648
PALMD	-7.28976	5.22E-19	6.92E-16	0.006391
MINOS1-NBL1	-7.27594	3.08E-05	5.10E-05	0.006452
ANPEP	-7.18996	6.87E-12	1.06E-10	0.006849
RANGRF	-7.13434	1.74E-15	2.16E-13	0.007118
FOSB	-7.07657	1.69E-15	2.16E-13	0.007409
ASB3	-7.0128	1.72E-15	2.16E-13	0.007743
EIF3CL	-7.0056	1.01E-16	2.74E-14	0.007782
ARHGAP8	-6.91659	1.20E-16	3.08E-14	0.008278
SCNM1	-6.77105	1.42E-16	3.38E-14	0.009156
BEST1	-6.7372	3.88E-18	2.99E-15	0.009373
PGAM4	-6.73178	1.87E-14	1.23E-12	0.009409
ARPC4-TTLL3	-6.71666	1.72E-18	1.44E-15	0.009508
SERF1A	-6.71602	6.55E-15	5.52E-13	0.009512
RASD1	-6.69425	3.50E-09	1.45E-08	0.009657
C11orf98	-6.66806	6.67E-18	4.06E-15	0.009834
BOLA2B	-6.62927	2.09E-10	1.44E-09	0.010102
TRIM69	-6.61179	1.58E-18	1.44E-15	0.010225
AREG	-6.54684	1.69E-14	1.14E-12	0.010696
SLC25A6	-6.48665	1.46E-16	3.40E-14	0.011151
CXCL8	-6.45005	1.59E-07	3.98E-07	0.011438
SCO2	-6.43349	3.50E-12	6.75E-11	0.01157
NEFL	-6.39927	3.20E-13	1.12E-11	0.011848

ESRP1	-6.33158	4.28E-14	2.41E-12	0.012417
MAGEA9	-6.28573	2.39E-13	9.01E-12	0.012818
KLHL23	-6.27142	3.99E-16	7.14E-14	0.012945
CCL20	-6.14373	4.39E-11	4.27E-10	0.014143
KRT6B	-6.06945	7.14E-11	6.19E-10	0.014891
TCN2	-6.0667	5.14E-11	4.81E-10	0.014919
NME2	-6.03089	1.34E-17	6.71E-15	0.015294
HIST2H2AA3	-6.01919	1.65E-15	2.14E-13	0.015419
UGT1A7	-5.99811	1.85E-05	3.17E-05	0.015645
IL3RA	-5.99549	6.51E-11	5.78E-10	0.015674
FAM72C	-5.97471	5.50E-18	3.91E-15	0.015901
ZBED1	-5.94794	1.01E-09	5.13E-09	0.016199
RPL36A	-5.91763	8.30E-18	4.62E-15	0.016543
GTPBP6	-5.84808	8.02E-15	6.44E-13	0.01736
UGT1A5	-5.82704	6.88E-18	4.06E-15	0.017615
CRABP2	-5.76694	2.33E-17	1.06E-14	0.018364
HCLS1	-5.75993	1.70E-16	3.62E-14	0.018454
EPGN	-5.7048	9.76E-18	5.15E-15	0.019173
RPS17	-5.6637	8.70E-12	1.27E-10	0.019727
DUSP1	-5.62958	1.98E-16	3.90E-14	0.020199
COX16	-5.55773	4.06E-17	1.63E-14	0.02123
TGM2	-5.52627	2.05E-16	3.95E-14	0.021698
TCN1	-5.47175	7.47E-12	1.14E-10	0.022534
HIST1H4J	-5.47103	6.01E-17	2.08E-14	0.022545
C10orf10	-5.45834	4.34E-14	2.42E-12	0.022745
IL1A	-5.44553	8.99E-17	2.58E-14	0.022947
NCF1	-5.44491	5.71E-08	1.62E-07	0.022957
FNTB	-5.42592	1.01E-16	2.74E-14	0.023261
EGR4	-5.41578	2.78E-12	5.68E-11	0.023425
POLR2J2	-5.41533	2.06E-15	2.41E-13	0.023433
UBE2V1	-5.40721	2.83E-09	1.22E-08	0.023565
PI3	-5.40412	1.89E-16	3.86E-14	0.023616
RASIP1	-5.3972	5.32E-14	2.84E-12	0.023729
KLHL13	-5.39076	1.67E-17	7.96E-15	0.023835
FLNC	-5.28802	0.000328	0.000478	0.025595
STBD1	-5.22768	5.67E-15	4.99E-13	0.026688
BMI1	-5.22483	2.58E-15	2.78E-13	0.026741
WFDC2	-5.2203	7.68E-14	3.78E-12	0.026825
AKAP17A	-5.209	9.41E-08	2.50E-07	0.027036
MTHFS	-5.20699	6.45E-17	2.14E-14	0.027073
PTGS2	-5.20573	2.73E-17	1.14E-14	0.027097
NR4A1	-5.11197	2.36E-15	2.62E-13	0.028916
PADI3	-5.09488	9.45E-16	1.46E-13	0.029261
PET117	-5.07902	1.07E-13	4.93E-12	0.029584
GPR68	-5.0578	1.33E-16	3.33E-14	0.030023
TUBB2B	-5.01872	5.21E-15	4.71E-13	0.030847
DUSP5	-5.00489	1.71E-15	2.16E-13	0.031144
SERPINB3	-4.98189	5.52E-17	1.98E-14	0.031645
HES1	-4.96026	4.65E-17	1.79E-14	0.032123
KLHDC8B	-4.95371	6.56E-06	1.21E-05	0.032269

NDUFC2	-4.91483	8.39E-17	2.47E-14	0.03315
TBC1D7	-4.90998	1.07E-13	4.93E-12	0.033262
ATP6V1C2	-4.90216	8.27E-11	6.97E-10	0.033443
NUPR1	4.894718	1.37E-16	3.35E-14	29.74794
RAB43	-4.86075	3.40E-15	3.32E-13	0.034417
EDN1	-4.84283	7.04E-17	2.14E-14	0.034847
CENPS	-4.78894	7.71E-14	3.78E-12	0.036173
SULT1A3	-4.7502	4.63E-16	8.01E-14	0.037157
CYR61	-4.74851	1.67E-16	3.62E-14	0.037201
C8orf76	-4.73514	2.21E-14	1.38E-12	0.037548
JUN	-4.71392	1.60E-16	3.62E-14	0.038104
PTGER4	-4.71267	8.41E-10	4.43E-09	0.038137
SULT1A4	-4.66239	9.02E-16	1.41E-13	0.039489
HIST2H4A	-4.62945	6.75E-12	1.05E-10	0.040401
ANKHD1	-4.61248	1.04E-12	2.67E-11	0.04088
SOCS3	-4.61118	1.66E-16	3.62E-14	0.040916
PAK6	-4.60251	4.45E-16	7.83E-14	0.041163
ZNF595	-4.57809	9.75E-15	7.58E-13	0.041866
ITGBL1	-4.5587	2.56E-15	2.78E-13	0.042432
HSPE1	-4.54845	1.28E-15	1.79E-13	0.042735
RFLNB	-4.53541	2.72E-16	5.10E-14	0.043123
CXCL2	-4.53439	3.69E-16	6.74E-14	0.043153
ANG	-4.52373	2.75E-16	5.10E-14	0.043473
TIAF1	-4.51476	1.04E-07	2.74E-07	0.043744
ABCC2	4.485308	1.73E-16	3.62E-14	22.39815
HOXB9	-4.47886	4.27E-14	2.41E-12	0.044847
STX11	-4.47198	1.96E-16	3.90E-14	0.045061
STN1	-4.4492	1.02E-15	1.52E-13	0.045778
SERPINB4	-4.39734	1.22E-15	1.74E-13	0.047453
TRIM31	-4.39636	1.20E-15	1.74E-13	0.047486
ATF3	-4.32705	5.97E-15	5.12E-13	0.049823
ANKRD22	-4.295	9.70E-13	2.53E-11	0.050942
NMB	-4.2629	3.23E-09	1.36E-08	0.052088
MAGEA9B	-4.19126	2.84E-15	2.97E-13	0.05474
FSTL1	-4.19011	5.61E-08	1.59E-07	0.054784
CPM	-4.17539	3.59E-11	3.65E-10	0.055345
TRIM15	-4.1393	2.92E-13	1.05E-11	0.056748
SNAI1	-4.11788	2.13E-15	2.46E-13	0.057596
KRT19	4.110375	4.97E-16	8.44E-14	17.27214
NACAD	-4.1026	3.57E-12	6.79E-11	0.058209
SAT1	-4.07864	1.11E-15	1.63E-13	0.059184
ASMTL	-4.06032	1.00E-05	1.78E-05	0.059941
TNFAIP3	-4.03962	5.48E-16	9.15E-14	0.060807
PABPN1	-3.97655	9.75E-16	1.48E-13	0.063524
LRG1	-3.96264	8.61E-16	1.41E-13	0.06414
HBEGF	-3.9626	8.96E-16	1.41E-13	0.064142
HOXD13	-3.96018	3.30E-15	3.27E-13	0.064249
PTP4A3	-3.95597	1.48E-15	1.98E-13	0.064437
GNA15	-3.95035	2.70E-15	2.85E-13	0.064688

EMC10	3.922143	8.88E-16	1.41E-13	15.15942
PAM16	-3.90375	9.63E-11	7.86E-10	0.066812
F8A3	-3.88754	1.27E-13	5.57E-12	0.067567
KLF2	-3.8863	2.60E-15	2.78E-13	0.067625
POLR2M	-3.88229	4.66E-15	4.25E-13	0.067813
HNRNPH1	3.876241	4.60E-15	4.23E-13	14.68469
GAST	-3.87304	7.44E-08	2.04E-07	0.06825
MALL	-3.86881	1.95E-15	2.33E-13	0.06845
ERCC5	-3.85011	1.32E-15	1.81E-13	0.069343
PLA2G4D	-3.84755	8.40E-13	2.28E-11	0.069466
PTX3	-3.82417	2.03E-09	9.25E-09	0.070601
PCBD1	-3.81249	2.98E-15	3.05E-13	0.071175
CKLF	-3.81037	9.13E-15	7.15E-13	0.07128
DUSP2	-3.79958	1.84E-15	2.26E-13	0.071815
RASA4B	-3.79511	1.72E-14	1.15E-12	0.072037
CYP24A1	-3.7806	3.68E-11	3.71E-10	0.072765
ARHGEF35	-3.7607	1.63E-15	2.14E-13	0.073776
ACY1	-3.75662	1.32E-14	9.26E-13	0.073985
RHOV	-3.74589	1.46E-15	1.98E-13	0.074537
PLAU	-3.73668	1.27E-15	1.79E-13	0.075015
LAPTM5	-3.71378	1.49E-13	6.34E-12	0.076215
ZHX1-C8orf76	-3.68453	1.24E-13	5.50E-12	0.077776
ANKRD2	-3.67002	1.14E-11	1.53E-10	0.078562
TSR2	-3.66298	3.60E-15	3.43E-13	0.078947
TXNIP	-3.66066	1.94E-15	2.33E-13	0.079074
CPZ	-3.64094	7.82E-12	1.17E-10	0.080162
ARHGEF25	-3.63185	1.03E-14	7.75E-13	0.080669
B2M	3.620192	1.22E-07	3.15E-07	12.29664
BTG2	-3.6194	2.20E-15	2.50E-13	0.081368
SLC2A3	-3.61875	2.05E-15	2.41E-13	0.081404
PTGS1	-3.61568	2.96E-15	3.05E-13	0.081578
FOSL1	-3.60829	3.07E-15	3.08E-13	0.081997
DCUN1D5	-3.60732	5.80E-15	5.06E-13	0.082052
SHISA2	-3.59855	3.52E-15	3.39E-13	0.082552
NECTIN4	-3.58793	3.41E-15	3.32E-13	0.083162
CCL5	-3.57833	3.46E-10	2.16E-09	0.083717
ARC	-3.57214	2.08E-14	1.32E-12	0.084077
MILR1	-3.55563	6.46E-13	1.87E-11	0.085045
PPAN	-3.55514	2.25E-13	8.60E-12	0.085074
MAP3K13	-3.54551	2.48E-15	2.73E-13	0.085644
PHF11	-3.54326	9.15E-14	4.31E-12	0.085777
UGT1A1	-3.53746	4.78E-12	8.25E-11	0.086123
GALM	-3.53178	6.12E-15	5.20E-13	0.086463
CP	-3.53148	1.26E-14	8.92E-13	0.086481
EDN2	-3.52689	2.09E-14	1.32E-12	0.086756
ANKRD37	-3.52346	4.48E-12	7.97E-11	0.086963
IL32	-3.51521	3.98E-15	3.69E-13	0.087461
BOLA2-SMG1P6	-3.51087	2.48E-14	1.53E-12	0.087725
RPL17	-3.50951	1.00E-14	7.67E-13	0.087808

MCTS1	-3.50551	3.07E-15	3.08E-13	0.088052
EIF3C	-3.50347	6.94E-15	5.80E-13	0.088176
RASA4	-3.49088	3.88E-11	3.86E-10	0.088949
APLN	-3.47743	3.82E-14	2.19E-12	0.089782
NGFR	-3.47464	7.25E-15	6.01E-13	0.089956
NR4A2	-3.4728	1.05E-11	1.45E-10	0.090071
HPRT1	-3.47053	1.03E-14	7.75E-13	0.090213
GSTT2B	-3.45554	1.05E-08	3.68E-08	0.091155
DDTL	-3.44884	7.92E-15	6.41E-13	0.091579
HCAR3	-3.43277	1.07E-14	7.81E-13	0.092605
FAM103A1	-3.4285	1.13E-14	8.24E-13	0.092879
HIST2H4B	-3.42378	6.58E-07	1.45E-06	0.093183
NRARP	-3.4167	3.79E-15	3.58E-13	0.093642
TXNDC5	3.401279	3.22E-11	3.34E-10	10.56542
STAP2	-3.39673	3.22E-09	1.36E-08	0.094947
TEX19	-3.39347	5.71E-13	1.73E-11	0.095162
DKK1	-3.38476	5.60E-15	4.97E-13	0.095738
NKX1-2	-3.37881	2.06E-14	1.32E-12	0.096134
PPP4R4	-3.37224	5.30E-15	4.75E-13	0.096573
CRIPT	-3.36609	7.41E-15	6.06E-13	0.096985
TRIB1	-3.36163	1.26E-14	8.92E-13	0.097286
CDC42EP2	-3.35005	5.03E-13	1.58E-11	0.09807
GLT8D2	-3.34912	4.20E-12	7.70E-11	0.098133
CEL	-3.34834	6.14E-13	1.82E-11	0.098186
TSTD3	-3.34486	3.25E-14	1.93E-12	0.098423
NFKBIZ	-3.33683	9.84E-15	7.59E-13	0.098972
SLX1B	-3.33146	5.54E-05	8.89E-05	0.099341
S1PR1	-3.32367	2.98E-14	1.80E-12	0.099879
GLIPR1	-3.31468	1.66E-13	6.81E-12	0.100503
CENPW	-3.31119	8.12E-15	6.46E-13	0.100747
AMTN	-3.29422	2.51E-12	5.24E-11	0.101939
CLN3	3.290261	6.17E-14	3.23E-12	9.782894
NDUFS7	3.283334	1.77E-14	1.18E-12	9.736031
NOMO3	-3.25991	1.05E-14	7.78E-13	0.104393
H1F0	-3.24755	7.43E-15	6.06E-13	0.105291
PPP1R15A	-3.24338	8.29E-15	6.54E-13	0.105595
UQCRQ	-3.2364	3.68E-14	2.12E-12	0.106107
ZC3H12A	-3.22712	1.39E-14	9.61E-13	0.106793
GEMIN8	-3.22489	3.04E-14	1.83E-12	0.106957
FAM86B1	-3.21492	6.59E-13	1.90E-11	0.107699
EPN1	3.213111	4.68E-14	2.54E-12	9.273481
CMC4	-3.21279	4.46E-14	2.46E-12	0.107859
PIGT	3.20815	2.47E-14	1.53E-12	9.241649
SGK1	-3.20163	4.43E-14	2.46E-12	0.108696
FAM72D	-3.19646	6.77E-14	3.50E-12	0.109086
DDN	-3.19461	3.37E-14	1.96E-12	0.109226
ANXA10	-3.18371	5.63E-12	9.23E-11	0.110054
EGLN2	3.18161	1.59E-14	1.08E-12	9.073189
SPRR1B	-3.16895	3.67E-10	2.26E-09	0.111186

COPZ2	-3.16787	2.33E-13	8.84E-12	0.111269
ATP6AP2	3.144001	1.07E-14	7.81E-13	8.839721
IL1B	-3.13912	3.06E-14	1.83E-12	0.113509
H2AFJ	-3.13828	1.05E-14	7.78E-13	0.113576
TMSB10	-3.13754	7.67E-14	3.78E-12	0.113633
ZNF131	3.132874	2.60E-14	1.59E-12	8.771807
RHOB	-3.13183	1.36E-14	9.46E-13	0.114085
C1QTNF6	-3.13151	7.98E-08	2.17E-07	0.11411
SDC4	-3.10672	1.25E-14	8.92E-13	0.116087

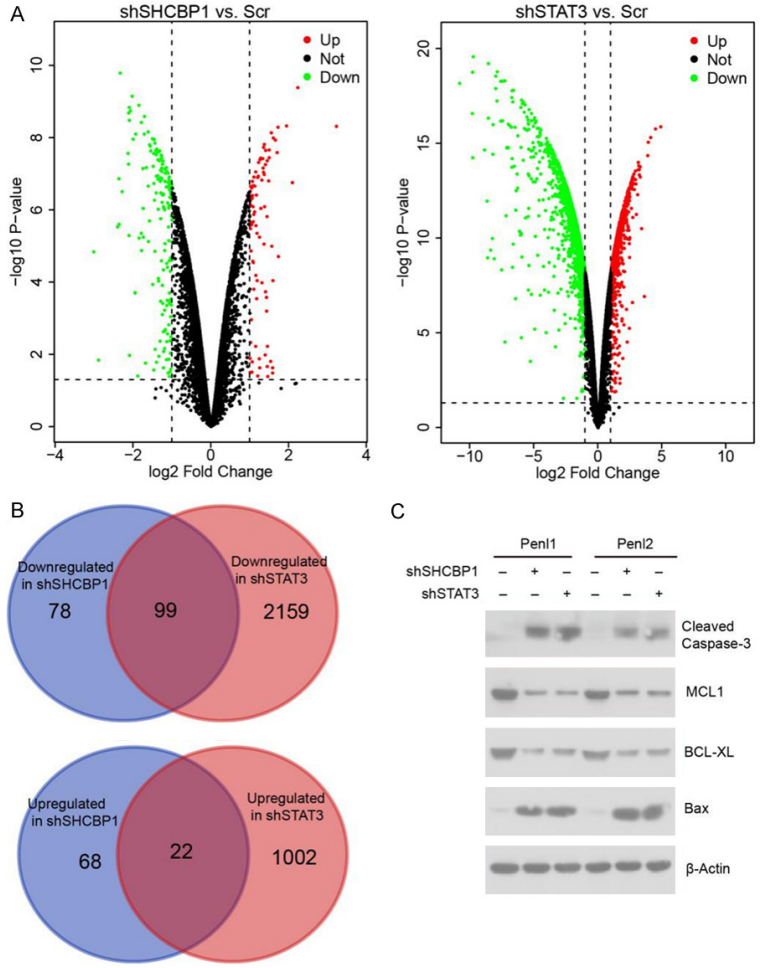

Figure S2. A. Volcano plot showing differentially expressed genes (DEGs) in Penl2 cells with SHCBP1 or STAT3 depletion. B. Commonly expressed DEGs in in Penl2 cells with SHCBP1 or STAT3 depletion. C. Expression of pro-apoptosis (cleaved caspase-3, BAX) and anti-apoptosis (MCL1, BCL-XL) genes in Penl1and Penl2 cells with SHCBP1 or STAT3 depletion.